Structural Engineering and Mechanics, *Vol. 65, No. 6 (2018) 657-678*
DOI: https://doi.org/10.12989/sem.2018.65.6.657

Development of super convergent Euler finite elements for the analysis of sandwich beams with soft core

V Sudhakar[2a], S Gopalkrishnan*[1] and K Vijayaraju[2b]

[1]*Department of Aerospace Engineering, Indian Institute of Science, Bangalore 560012, India*
[2]*Aeronautical Development Agency, PB No:1718, Vimanapura Post, Bangalore 560017, India*

(Received April 27, 2017, Revised January 5, 2018, Accepted January 10, 2018)

Abstract. Sandwich structures are well known for their use in aircraft, naval and automobile industries due to their high strength resistance with light weight and high energy absorption capability. Sandwich beams with soft core are very common and simple structures that are employed in day to day general use appliances. Modeling and analysis of sandwich structures is not straight forward due to the interactions between core and face sheets.

In this paper, formulation of Super Convergent finite elements for analysis of the sandwich beams with soft core based on Euler Bernoulli beam theory are presented. Two elements, Eul4d with 4 degrees of freedom assuming rigid core in transverse direction and Eul10d with 10 degrees of freedom assuming the flexible core were developed are presented. The formulation considers the top, bottom face sheets and core as separate entities and are coupled by beam kinematics. The performance of these elements are validated by results available in the published literature. Number of studies are performed using the formulated elements in static, free vibration and wave propagation analysis involving various boundary and loading conditions. The paper highlights the advantages of the elements developed over the traditional elements for modeling of sandwich beams and, in particular wave propagation analysis.

Keywords: sandwich beams; face sheets; core; governing equations; finite element method; super convergence; static analysis; free vibration; wave propagation; composite or metallic face sheets

1. Introduction

Sandwich material constructions are employed in the design of structures due to their light weight and high energy absorption capability. Due to their ability for the tailor-made design with combination of face sheets and core sections to meet the given load conditions, these structures find their use in many applications. The face sheets will be taking the load and connected to other structural members, while the soft-core material, will be used to absorb energy during impact like situation. Cores generally play very crucial role in achieving the desired properties of sandwich structures, either through geometric arrangement or material properties or both. Foams are in extensive use nowadays as core material due to the ease in manufacturing and their low cost. Hence, the analysis of sandwich constructions has attracted the attention of many researchers.

There are two different approaches to model sandwich structures, one is called Equivalent Single Layer (ESL) theory and the second is called layer wise theory. In the former method, core and face sheets are synthesized as a single entity and the average properties of the hybrid structure are obtained using macro mechanics approach as is done in the analysis of laminated composites. In the second approach, each layer (in this case face sheets and core) are considered as separate entity and are synthesized using approximate beam or plate kinematics at the interfaces. In this paper, we adopted second approach, where the face sheets and core are modeled separately and they are synthesized using appropriate kinematics at the interface, that is the load transfer from face sheets to core is either by pure shear (in case of incompressible core) or through shear and normal stresses (in the case of compressible core).

1.1 Literature survey

Many analytical models assume that the core do not carry bending stresses and the core deformation is only due to shear. Such a theory is a possibility if the face sheets are modelled using Euler-Bernoulli beam assumption. If the axial and transverse displacements in the core are assumed as linear function of thickness, such an assumption requires that the normal stress in the core be constant and the face sheets be modelled using First order Shear Deformation Theory(FSDT). Many researchers Frostig (1992, 1994, 2003), Marur and Kant (1996), Yang *et al*. (2005), Zhen *et al*. (2008), Yang *et al*. (2007) have used the axial and transverse displacements variation in the core. In the model proposed by Allen and Howard (1969) it is assumed that there is only a bending deformation in the face sheet and thus in plane deformations are null. On the other hand, the model proposed by Frostig (2003) assumes that the plane section of the core remains vertical and there are both the in-plane as well as bending displacements in the face

*Corresponding author, Professor
E-mail: krishnan@iisc.ac.in

http://www.techno-press.com/journals/sem&subpage=7 ISSN: 1225-4568 (Print), 1598-6217 (Online)

sheets. Frostig (2003) discusses two theories for modelling sandwich structures, namely Ordinary Sandwich Panel Theory(OSPT) and High order Sandwich Panel Theory(HSAPT). The OSPT model is based on the assumption that the plane of section of core and faces remain plane after deformation however the slopes are different, while HSAPT is a closed form higher order computational model. OSPT model assumes a linear variation of deflection through the thickness for the face sheets and core while HSAPT model assumes higher order variation, which represents the compressible effects of core. Frostig and Baruch (1994) in their higher order approach for the free vibration analysis of sandwich beams, considered the skins as elementary beams with axial and bending resistance and only shear behavior in the core with zero normal transverse stress. Catherine *et al*. (2012) presented an analysis of sandwich beams with a compliant core and with in-plane rigidity Extended High-Order Sandwich Panel Theory (EHSAPT), in which the compressibility of the soft core in the transverse direction is also considered. And the transverse displacement in the core is of second order in the transverse coordinate and the in-plane displacements are of third order in the transverse coordinate.

Zhen (2008) made an effort to compare several displacement-based theories such as Global Local Higher order Theory (GLHT), Zig Zag Theory(ZZT), Higher order Shear Deformation Theories(HSDT) and First order Shear Deformation Theory(FSDT). In HSDT itself, there are many theories which differs based on the number of unknown variables. GLHT proposed by Li and Liu (1997), *a-priori* satisfies displacements and transverse shear stresses continuity conditions at interfaces. Displacement fields are approximated using a set of functions which are functions of material, sectional properties and thickness with six number of unknown variables. In ZZT proposed by Cho and Parameter (1993), the condition of transverse shear stress continuity at interfaces for general lamination configurations is satisfied by superimposing a cubic varying displacement field on a *zig-zag* linear displacements. A comparative study on the use of Zigzag functions in equivalent single layer theories for laminated composite and sandwich beams was presented by Marco (2013). To approximate the three-dimensional elasticity problem to a two-dimensional plate problem, Matsunaga (2001) has proposed a higher order shear deformation theory *HSDT*-98, where the displacement fields can be expressed as a Taylor's series in terms of thickness coordinate. The in-plane displacement field of *HSDT-98* consists of ninth order polynomial in global thickness coordinate '*z*' whereas the transverse deflection is represented by an eighth order polynomial of z with total number of unknowns being 19 in this model. In *HSDT*-76, the axial deformation is approximated as 7^{th} order polynomial in thickness coordinate and the transverse displacement is approximated as sixth degree polynomial with 15 unknowns in this model. Kant and Swaminathan (2001) reported a HSDT, called *HSDT*-33, where both axial and transverse displacements were approximated by a quadratic variation in thickness coordinates and total number of unknown variables are 8 in this case. Each of these theories gave the results of varying accuracy. Reddy (1984) proposed a higher order shear deformation theory (called *HSDT-Reddy*) which can satisfy the transverse shear stress free boundary conditions, only includes 3 unknown variables. Damanpacka and Khalilia (2012) proposed high-order free vibration analysis of sandwich beams with a flexible core using dynamic stiffness method.

Modeling of sandwich beams using the conventional FE software is not simple as the direct sandwich beam elements are not available. Efforts were made by Yang *et al*. (2007) to model sandwich beams in ABAQUS using 2D beams for face sheets and 3D elements for core. Ivaez *et al*. (2010) developed a numerical model to analyze the dynamic flexural behaviour of composite foam-core sandwich beams, using ABAQUS for modeling foam core as crushable and explicit code for modeling the face sheet behavior. Gillich *et al*. (2014) made an effort to evaluate the severity of localization of transversal cracks in sandwich beams. Efforts on the experimental studies on sandwich beams were also reported in literature. Experimental studies on clamped sandwich beams subjected to impact loading by Zhihua *et al*. (2011), free vibration of a three-layered sandwich beam by Banerjee *et al.* (2007), and prediction of the dynamic response of composite sandwich beams under shock loading by Tagarielli *et al*. (2010), were also reported. Poortabib and Maghsoudi (2014) investigated linear buckling analysis of a curved sandwich beam with a flexible core by deriving the equations for face sheets via the classical theory of curved beam, whereas for the flexible core, the elasticity equations in polar coordinates are implemented. Nonlinear magneto-electro-mechanical free vibration behavior of rectangular double-bonded sandwich micro beams based on the modified strain gradient theory (MSGT) is investigated by Mohammadimehr and Shahe (2016). Three-dimensional nonlinear finite element model was developed by Yan *et al*. (2015) for the ultimate strength analysis of such Steel Concrete Steel sandwich composite beams. Cunedioglu (2015) adopted multi layered approach for modeling of an edge cracked symmetric sandwich beam made of functionally graded materials, based on linear elastic fracture mechanics theory, considered within the Timoshenko first order shear deformation beam theory(FSDT) by using finite element method.

In case of sandwich structures, the interface stresses between the face sheets and core, shear stress, τ_{xz} and normal transverse stress, σ_{zz} are the key parameters. As the depth of the structure increases, shear strain and the transverse normal strains will be considerable and thus shear deformation along with stretching effect will become crucial. Many theoretical models based on shear deformation were proposed for the analysis of the sandwich beams or plates made of functionally graded materials. Among them, Four variable refined plate theory, displacement based Higher order Shear Deformation Theory (HSDT) which includes undetermined integral terms, Hyperbolic shear deformation theory and Refined Trignometric Shear Deformation Theory (RTSDT) were found to be used by the researchers for many applications. Meiche *et al.* (2011) presented a new hyperbolic shear deformation theory for the buckling and free vibration analysis of thick functionally graded sandwich plates taking into account transverse shear deformation effects. The theory assumes the transverse shear stresses vary parabolically across the thickness and the closed-form solutions of functionally graded sandwich plates are obtained using the Navier solution. Meziane *et al.* (2014) selected the displacement field in their refined shear deformation theory based on nonlinear variations in the in-plane displacements through the thickness of the plate, by dividing the transverse displacement into the bending and shear parts. They presented the results of critical buckling loads of several types of symmetric exponentially graded material sandwich plates. Ahmed *et al.* (2016) proposed a new HSDT for bending and free vibration analysis for functionally graded plates, which deals with only three unknowns as classical plate theory including sinusoidal variation of transverse shear strains through the thickness of the plate theory. In an efficient shear deformation theory developed by Ahmed *et al.* (2016) for wave propagation of a functionally graded material plate, the number of unknowns and governing equations are reduced, by dividing the transverse displacement into bending and shear parts. Also, the physical neutral surface concept was adopted and hence, there is no stretching, bending coupling effect. Using the same theory of neutral surface-based formulation and assuming FSDT, Bellifa *et al.* (2016) carried out the bending and free vibration analysis of functionally graded plates.

Few researchers attempted the analysis of functionally graded beams with porosities, variation of materials properties of face sheets and core to capture the practical cases closely. Abdelaziz *et al.* (2011) adopted the four-variable refined plate theory for the static response of functionally graded sandwich plates, where they considered the sandwich with functionally graded face sheet and homogeneous core and the sandwich with homogeneous face sheet and functionally graded core. Abdelaziz *et al.* (2017) reported the application of same theory for the bending, vibration and buckling of powerly graded material (PGM) sandwich plate with various boundary conditions. Fard (2014) proposed HSDT for free vibration of sandwich curved beams with a functionally graded core. Atmane Hassen Ait *et al.* (2015) presented a free vibrational analysis of functionally graded beams with porosities, with a simple displacement field based on HSDT, in which the transverse displacements consist of bending and shear components, but both will not contribute to each other. Remarkable efforts by Ait *et al*. (2015) reported for wave propagation in functionally graded plates with porosities using various higher-order shear deformation plate theories. The rule of mixture is modified to describe the material properties with porosity phases and the analytic dispersion relation of the functionally graded plate is obtained by solving an eigenvalue problem. Lazreg *et al*. (2016) presented a new displacement based high-order shear deformation theory for static and free vibration analysis of functionally graded beams and the material properties of the functionally graded beam are assumed to vary according to power law distribution of the volume fraction of the constituents.

Some of the theories considered the effect of stretching with reference the sandwich beams and plates, by taking the normal transverse strain into the formulation. Hebali *et al.* (2014) developed a new quasi-three-dimensional hyperbolic shear deformation theory for the bending and free vibration analysis of functionally graded plates by dividing the transverse displacement into bending, shear, and thickness stretching parts. Belabed *et al*. (2014) presented an efficient and simple higher order shear and normal deformation theory for functionally graded material (FGM) plates. This theory accounts for both shear deformation and thickness stretching effects by a hyperbolic variation of all displacements across the thickness. Mahi *et al*. (2015) used the same theory for bending and free vibration analysis of isotropic, functionally graded, sandwich and laminated composite plates. Mohamed *et al*. (2015) presented a simple and refined trigonometric higher-order beam theory for bending and vibration of functionally graded beams, in which the inclusion of thickness stretching effect ($\varepsilon \neq 0$) and this effect on the deflections, stresses were clearly highlighted. Riadh *et al. (*2015) proposed a new refined hyperbolic shear and normal deformation beam theory to study the free vibration and buckling of functionally graded sandwich beams under various boundary conditions. And the effects of transverse shear strains as well as the transverse normal strain are taken into account and the effects of thickness stretching, boundary conditions, and thickness to length ratios were discussed. Bennoun *et al*. (2016) proposed a novel five-variable refined plate theory, by considering the transverse displacement with contributions of bending, shear, and thickness stretching parts and also accounts for hyperbolic distribution of the transverse shear strains. Free vibration analysis of functionally graded sandwich plates, FGM face sheet and homogeneous core and the sandwich with homogeneous face sheet and FGM core were analyzed using this theory and observed a good match with 3D elasticity solutions and higher order theories. Fatima *et al*. (2016) presented a zeroth-order shear deformation theory for free vibration analysis of functionally graded (FG) nanoscale plates resting on elastic foundation, considering the influences of small scale and the parabolic variation of the transverse shear strains across the thickness of the nanoscale plate. The effect of transverse shear deformation is included in the axial displacements by using the shear forces instead of rotational displacements as in available high order plate theories.

Application of these theories were not limited to structures. Some of the works published by the researchers were found in the area of thermal analysis. Tounsi *et al*. (2013) considered the transverse shear deformation effects (by following RTSDT) for the thermo-elastic bending analysis of functionally graded sandwich plates. They studied the influences played by the transverse shear deformation, thermal load, plate aspect ratio, and volume fraction distribution on the deflections and stresses of functionally graded metal-ceramic plates. Bachir *et al*. (2013) reported the thermo-mechanical bending response of functionally graded plates resting on Winkler-Pasternak elastic foundations based on RTSDT. Hamidi *et al*. (2015) presented a simple but accurate sinusoidal plate theory for the thermo-mechanical bending analysis of functionally graded sandwich plates, incorporating the thickness stretching effect. Bachir *et al*. (2016) proposed a simple shear deformation theory for thermal stability of functionally graded sandwich plates and reported that the obtained numerical results achieved are on par with conventional FSDT which has more unknowns. Bousahla *et al*. (2016) developed a four-variable refined plate theory for buckling analysis of functionally graded plates subjected to uniform, linear and nonlinear temperature rises across the thickness direction to investigate the variation of coefficient of thermal expansion. Abdelbaki *et al.* (2017) recently proposed a simplified HSDT for thermal buckling analysis of cross-ply laminated plates in which the displacement field introduces undetermined integral terms and contains only four unknowns. El-Haina *et al*. (2017) presented a simple analytical approach to investigate the thermal buckling behavior of thick functionally graded sandwich by employing both the sinusoidal shear deformation theory and stress function. Menasria *et al.* (2017) used a new displacement field that includes undetermined integral terms for analyzing thermal buckling response of functionally graded (FG) sandwich plates by considering a trigonometric variation of transverse shear stress and verifies the traction free boundary conditions without employing the shear correction factors. Using the same theory, Bellifa *et al*. (2017) proposed a methodology for buckling analysis of functionally graded plates and they determined the closed-form solutions of rectangular plates.

It can be found out that the numerous efforts were made for the analysis of sandwich structures and the classical to mixed formulations to novel methodologies were proposed. All these efforts can be noted basically based on the shear deformation and stretching effect as they play a crucial role. In the present study, efforts were made to develop the elements without and with this stretching effect basically to quantify their effect while transferring the energy from core to the face sheets which will reflect on the overall performance. And the shear effects are captured using FSDT in face sheets.

1.2 Concerns and possible solutions

All of these theories consider governing differential equations of varying complexity, which requires numerical techniques such as Finite Element Method (FEM) to solve. Most of the theories consider the weak formulation and not the strong form, while deriving the governing equations. The degree of accuracy of results depends on the ability of the chosen interpolation polynomials of the finite elements to satisfy the governing equations as closely as possible. Many finite elements suffer from problems such as shear locking, poor convergence, etc. due to inappropriate interpolation functions. In fact, if a proper interpolating functions are chosen, even FEM based FSDT will give accurate results. Hence, we will use this approach to formulate a family of finite elements based on FSDT for sandwich structures, in which the interpolating polynomial of the formulated FEM satisfy the static part of the governing equation. Hence, such an element will give exact results for the static analysis under point loads, while the dynamic analysis will still be approximate due to inaccurate inertial distribution. However, since the static part of the governing equation is exact, the convergence of results provided by this element is expected to be superior compared to conventional FEM. Hence, this formulation is normally referred to as Super Convergent FE formulation.

Energy absorption studies requires deep understanding of wave propagation, which is a multimodal phenomenon, where all higher modes will get excited to a short duration load. The frequency content of such load will be large. At these large frequencies, the wavelength will be very small and hence for accurate results, conventional finite elements mesh size should be comparable with the wavelength and it should be typically one eighth or one tenth of wavelengths. Hence, mesh sizes for wave propagation problems is very high requiring new methodologies to reduce problem size. Spectral FEM (Gopalakrishnan *et al*. 2008) is one such method, while Super Convergent FEM which is a topic of this paper, is the other. Since, the stiffness is exactly captured in Super Convergent FE formulation, it is expected that this formulation requires smaller mesh sizes and superior convergence properties compared to conventional FEM and hence will be of great use in solving wave propagation problems.

Such formulation for higher order rod by Gopalakrishnan (2000), beam by Chakraborty *et al.* (2002), thin walled beam by Mitra *et al*. (2004), higher order composite beams by Murthy *et al.* (2005, 2007), Ghosh and Goplakrishnan (2007) have been reported in the literature. Through this procedure, the continuity and completeness of the displacement polynomial, which is essential to obtain shear locking free performance, can be achieved. Shear locking is the common phenomena in case of thin beams, where the beam slopes are not computed using the transverse displacements. Elimination of locking through the reduced order integration by making the shear stiffness matrix rank deficient is most widely used by Cook *et al.* (2002). As the present formulation employs the exact solutions as interpolation functions, the element is naturally free from locking. This super convergence property makes this element more powerful when compared to the other formulations, which provides higher rate of convergence and there by gives a great benefit to use less number of elements for carrying out the analysis of sandwich beams, especially for wave propagation studies. We (Sudhakar *et al*. 2010) reported the development of sandwich beam based on Timoshenko beam theory with partial compressible effects of core with super convergence property earlier.

1.3 Novelty of the present work and applications

Following novel points can make the elements presented in this paper superior over the other.

- use of the strong form of the governing differential equations in the element formulation
- use the solution of the differential equations as interpolation functions to make the stiffness matrix exact for the static case and shear locking free in case of thin beams
- element model assumes the degrees of freedom(dof) at the face sheets to facilitate realistic load application and boundary conditions
- effects of core are applied through kinematic relations with dof and forces respectively, which will provide freedom to capture the core phenomena many ways in compatible with face sheets
- metallic and /or composite face sheets

• Eul4d element considers the rigid core with uniform transverse displacement and slope

• Eul10d element considers the flexible core with effects of shear stress in longitudinal, transverse directions and also stretching in thickness direction.

As these elements are developed on the basis of Euler Bernouli beam theory with the specific features mentioned above, the applications where these elements can be used, can be many as listed below.

• Static, free vibration and wave propagation analysis of thin beams.

• Beams with loads leading to bending phenomena predominantly, say point loads, uniformly distributed loads.

• Analysis of beams with application of boundary conditions at top and bottom face sheets same or different-more rigid to more flexible.

• Use of Metallic or composite face sheets with wide variety of foam cores

Energy and vibration absorption studies of sandwich beams

This paper covers the general Super convergent element formulation outlining the procedure in next section. Later Element formulation for Eul4d, Eul10d with details of stiffness matrix derivation and static condensation for obtaining the solution. The developed elements are extensively validated for static, free vibration and wave propagation analysis problems as presented in following subsequent sections.

2. Super convergent finite element formulation

Euler beam theory is the basic beam theory for pure bending analysis, where the shear deformation is not considered and hence widely acceptable for thin beams. This element basically considers the contribution of core through shear stress, τ_{xz} and normal transverse stress, σ_{zz} at interfaces with face sheets so that the compressibility effects of core are captured. Incompressible as well as flexible effects of the core are considered and are captured by incorporating appropriate beam kinematics. The respective degrees of freedom considered in these super convergent finite element sandwich Euler Bernoulli beam elements developed, are listed as below.

• 4 degrees of freedom Euler Bernoulli element (Eul4d) :u_{0t} ,w, $\frac{dw}{dx}$, u_{0b}

• 10 degrees of freedom Euler Bernoulli element (Eul10d) u_{0t}, w_t, dw_t/dx, u_{0b}, w_b, dw_b/dx τ^t_{xz}, τ^b_{xz}, σ^t_{zz}, σ^b_{zz}.

Super Convergent formulation for higher order rods, beams are available in Gopalkrishnan (2000) to Ghosh and Goplakrishnan (2007). τ^c_{xz} is the shear stress in core, τ^t_{xz} and τ^b_{xz} are the shear stresses at top and bottom interfaces between the face sheet and core. For a constant shear stress variation across depth of core, τ^c_{xz} is used. While τ^c_{xz} varies across depth of core, τ^t_{xz} and τ^b_{xz} are used correspondingly to denote the shear stress. Similarly, σ^c_{zz} is the transverse normal stress in core. σ^t_{zz} and σ^b_{zz} denotes the transverse normal stresses in core at the top and bottom interfaces.

Among the elements developed, Eul4d element is the basic element that assumes rigid core, where the transverse displacement is constant throughout depth of the core. These elements can be employed for thin sandwich beams under bending loads. Eul10d is a higher order element which is expected to simulate the real conditions with flexible core represented through the shear stress and transverse normal stresses at top and bottom interfaces. General frame work for all these super convergent finite elements formulated based on Euler beam theory is presented in the next subsection.

2.1 Super convergent FE frame work for sandwich beam elements

The details such as governing equations, interpolation functions, etc. for each formulated element are given in the following sections. The general procedure for formulating super convergent sandwich beam element is outlined, which mainly explains the derivation of stiffness and mass matrices. All formulations will consider both top and bottom face sheets and core as separate entities. The face sheets are connected to core through interfacial shear and normal stress in the transverse direction depending upon the type of element formulated.

A generalized sandwich beam with face sheets, core and coordinate systems followed are as shown in Fig. 1(a). Based on the idealization of model with assumed kinematics in terms of degrees of freedom, the stress distribution in the element, external force acting on the element and the energy associated with the systems in various forms are calculated

Governing differential equations can be derived using Hamilton's principle, which are given by

$$\delta \int_{t_1}^{t_2} (T_t - U_t + W_t)dt = 0,$$

$$\delta \int_{t_1}^{t_2} (T_b - U_b + W_b)dt = 0$$

WhereT_t, T_brepresents the kinetic energy, U_t, U_b are the potential energy and W_t, W_b are the work done by the shear and transverse normal stress due to core corresponding to top and bottom face sheets respectively, which are given by

$$\begin{aligned} U_t &= \frac{1}{2}\int_0^L \int_{A_t} (\sigma^t_{xx}\,\epsilon^t_{xx} + \tau^t_{xz}\,\gamma^t_{xz})\,dx\,dA_t \\ U_b &= \frac{1}{2}\int_0^L \int_{A_b} (\sigma^b_{xx}\,\epsilon^b_{xx} + \tau^b_{xz}\,\gamma^b_{xz})\,dx\,dA_b \\ T_t &= \frac{1}{2}\int_0^L \int_{A_t} \rho_t(\dot{u}_t^2 + \dot{w}_t^2)dx\,dA_t, \\ T_b &= \frac{1}{2}\int_0^L \int_{A_b} \rho_b(\dot{u}_b^2 + \dot{w}_b^2)dx\,dA_b \\ W_t &= \frac{1}{2}\int_0^L b(\tau^c_{xz}u_t + \sigma^t_{zz}w_t)dx \\ W_b &= \frac{1}{2}\int_0^L b(\tau^c_{xz}u_b + \sigma^b_{zz}w_b)dx \end{aligned} \tag{1}$$

where dA_t =b dz_t and dA_b=bdz_b are the area of cross section of top and bottom face sheets under consideration.

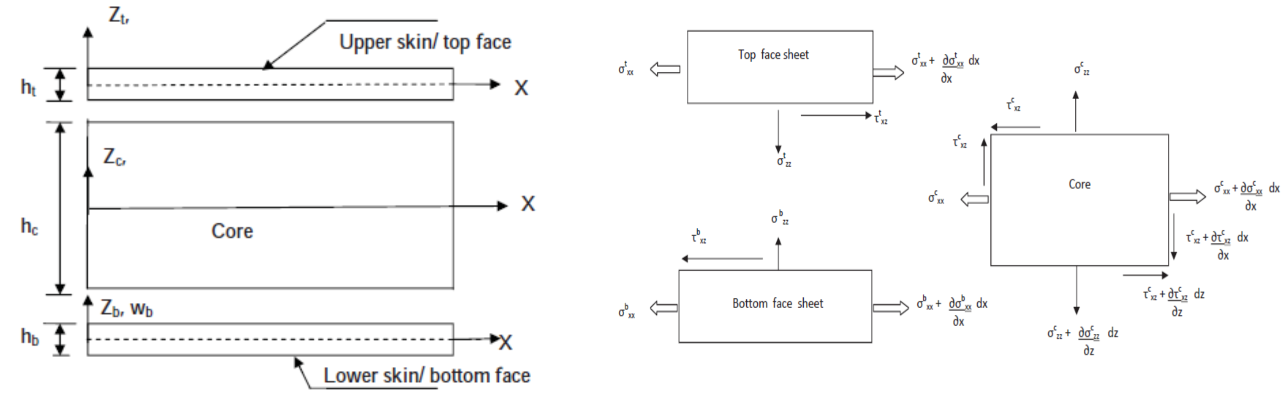

(a) Geometry Axis System (b) Forces, Stress Resultants

Fig. 1 Element: Axis System and Free Body Diagram

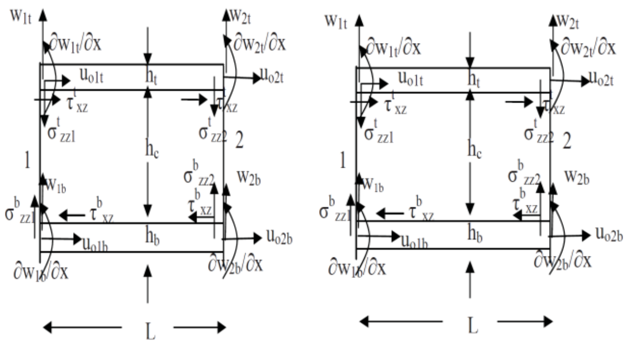

(a) Degrees of freedom (b)Forces, Stress Resultants

Fig. 2 Two noded 10 dof Sandwich beam element

Assuming FSDT, longitudinal displacements u_t, u_b are related as

$$u_t = u_{0t} - z_t \frac{dw_t}{dx},\ u_b = u_{0b} - z_b \frac{dw_b}{dx} \tag{2}$$

It is essential to note that the inertial mass contribution from core is not included as the degrees of freedom corresponding to core are not included directly in any of the formulations and hence, they are included through available degrees of freedom at top and bottom face sheets through lumping procedures. Based on the assumed idealization, that is the core is either rigid or flexible, the terms in the energy expression will be appropriately modified.

Once the governing equations are derived, the displacement functions need to be derived using super convergent formulation where the shape functions are obtained by solving static part of these governing equations exactly. Subsequently, using these shape functions, the stiffness matrix and mass matrix of the element will be derived.

2.2 Stiffness matrix

Stiffness matrix can be derived based on the strain displacement relations and expressed as,

$$[K^e]_{N\times N} = \int_0^L \int_0^b \int_{-\frac{h}{2}}^{\frac{h}{2}} \lfloor B \rfloor^T [C][B\ ]\ dz\, dy\, dx \tag{3}$$

Where $\lfloor K^e \rfloor$ denotes the element stiffness matrix, [B] denotes the strain displacement matrix, [C] denotes the material stress strain constitutive relation matrix. Element stiffness matrix will be computed for *N* degrees of freedom (dof), that the element can support. Free body diagram for the sandwich beam can be written as shown in Fig. 1(b), which is applicable for Eul10d.

Similar free body diagrams for Eul4d elements can be derived based on the degrees of freedom and stress resultants assumed respectively. The stresses are related to the strains using the constitutive relation and is given by

$$\begin{Bmatrix} \sigma_{xx} \\ \sigma_{zz} \\ \tau_{xz} \end{Bmatrix} = \begin{bmatrix} Q_{11} & 0 & 0 \\ 0 & Q_{22} & 0 \\ 0 & 0 & Q_{55} \end{bmatrix} \begin{Bmatrix} \epsilon_{xx} \\ \epsilon_{zz} \\ \gamma_{xz} \end{Bmatrix} \tag{4}$$

which can be written as

$$\{\sigma\} = \lfloor Q \rfloor\ \{\epsilon\} \tag{5}$$

For the top and bottom face sheets, the stresses and strains are calculated using these expressions, where Q_{ij} are the elements of the anisotropic constitutive matrix, where the effect of ply-angle is taken into consideration. Q_{ij} are evaluated using the expressions given by Vinson and Jack (1999). In addition to the shear stress τ_{xz}^t for top face sheet and $\tau_{xz}^b$for bottom face sheet, the core shear stress τ_{xz}^c and normal stress σ_{zz}^c will be acting at the interface of the core and the face sheets.

Formulation begins with evaluation of interpolation functions obtained using the static part of the solution of the governing equation. Here, the formulation procedure is illustrated with all possible dofs as listed below as the vector containing ten independent degrees of freedom, which can be written in a matrix form as

$$\{u\} = \left\{ \mathrm{u_{0t}}, \mathrm{w_t}, \frac{\partial w_t}{\partial x}, \mathrm{u_{0b}}, \mathrm{w_b}, \frac{\partial w_b}{\partial x}, \tau_{xz}^{t}, \tau_{xz}^{b}, \sigma_{zz}^{t}, \sigma_{zz}^{b} \right\}^T \tag{6}$$

Various possible degrees of freedom, free body diagram of forces and stresses are shown in Fig. 2.

We assume that there are n_t number of constants in the solution, which needs to be determined in order to define the functions completely and only 2 m of them are available as boundary conditions corresponding to dof, m. Hence, $n_x = n_t - 2\,m$ constants are not independent and they need to be expressed in terms of independent constants. By substituting the assumed polynomials from Eq. (6) into the governing equations, a set of equations will be obtained. Let the vector $\{ C_d \}$ be the vector of dependent constants and vector $\{C\_i\}$ be the vector of independent constants. Set of relations obtained can be put in matrix form, which can be expressed as

$$[A_1]_{n_x \times n_x}\ \{C_d\}_{n_x \times 1} = [A_2]_{n_x \times 2m}\ \{C_i\}_{2m\times 1} \tag{7}$$

where $[A_1], [A_2]$ are the matrices consists of the stiffness coefficients associated with $\{ C_d \}$ and $\{ C_i \}$ vectors. Care should be taken while selecting the dependent constants in matrix $\{C_d\}$ so that matrix $[A_1]$ will be non-singular.

From Eq. (7), $\{ C_d \}$ can be obtained as

$$\{C_d\}_{n_x \times n_x} = [A_1]^{-1}{}_{n_x \times n_x} [A_2]_{n_x \times 2m}\ \{C_i\}_{2m\times 1} \tag{8}$$

which can be written as

$$\{C_d\}_{n_x \times n_x} = [A_{di}]_{n_x \times 2m}\ \{C_i\}_{2m\times 1} \tag{9}$$

Next, the vector containing regular displacements can be written in terms of both dependent and independent constants by expressing the governing equations in matrix form as

$$\{u\}_{m\times 1} = [A_d]_{m\times n_x}\ \{C_d\}_{n_x \times 1} + [A_i]_{m\times 2m}\{C_i\}_{2m\times 1} \tag{5}$$

Substituting $\{C_d\}$ obtained from Eq. (8) in Eq. (10), we get the relationship as

$$\begin{aligned}\{u\}_{m\times 1} = [A_d]_{m\times n_x} [A_{di}]_{n_x\times 2m}\{C_i\}_{2m\times 1}\\ + [A_i]_{m\times 2m}\{C_i\}_{2m\times 1}\end{aligned} \tag{11}$$

The above equation can be written as follows.

$$\{u\}_{m\times 1} = [A_c]_{m\times 2m}\{C_i\}_{2m\times 1} \tag{12}$$

Where

$$\{A_c\}_{m\times 2m} = [A_d]_{m\times n_x} [A_{di}]_{n_x\times 2m} + [A_i]_{m\times 2m} \tag{13}$$

By substituting the boundary conditions at two nodes of an element at $x = 0$ and $x = L$ as shown in Fig. 2, we get a matrix relation between the constants and the nodal displacements, which can be written as

$$\{u^e\}_{2m\times 1} = [A_e]_{2m\times 2m}\{C_i\}_{2m\times 1} \tag{14}$$

Where $\{u^e\} = \{u_1, u_2\}^T$
and $\{u^e\}$ is the elemental degrees of freedom vector, $\{ u_1\}$ and $\{ u_2 \}$ are the vectors at nodes at $x = 0$ and j at $x = L$ defined as

$$\{u_1\} = \begin{Bmatrix} \mathrm{u_{0t1}}, \mathrm{w_{t1}}, \left(\dfrac{\partial w_t}{\partial x}\right)_1, \mathrm{u_{0b1}}, \mathrm{w_{b1}}, \left(\dfrac{\partial w_b}{\partial x}\right)_1, \\ \tau^{\mathrm{t}}_{\mathrm{xz1}}, \tau^{\mathrm{b}}_{\mathrm{xz1}}, \sigma^{\mathrm{t}}_{\mathrm{zz1}}, \quad \sigma^{\mathrm{b}}_{\mathrm{zz1}} \end{Bmatrix}^T$$

$$\{u_2\} = \begin{Bmatrix} \mathrm{u_{0t2}}, \mathrm{w_{t2}}, \left(\dfrac{\partial w_t}{\partial x}\right)_2, \mathrm{u_{0b2}}, \mathrm{w_{b2}}, \left(\dfrac{\partial w_b}{\partial x}\right)_2, \\ \tau^{\mathrm{t}}_{\mathrm{xz2}}, \tau^{\mathrm{b}}_{\mathrm{xz2}}, \sigma^{\mathrm{t}}_{\mathrm{zz2}}, \quad \sigma^{\mathrm{b}}_{\mathrm{zz2}} \end{Bmatrix}^T$$

From Eq. (14), we have

$$\{C_i\}_{2m\times 1} = [A_e]^{-1}{}_{2m\times 2m}\{u^e\}_{2m\times 1} \tag{15}$$

It is to be noted that unlike conventional finite elements, super convergent elements will give constants dependent on material as sectional properties of an element. Displacements at any point in the element are related to the nodal displacements using the shape functions [*N*], which can be obtained as follows

$$\{u\}_{m\times 1} = [A_c]_{m\times 2m} [A_e]^{-1}{}_{2m\times 2m}\{u^e\}_{2m\times 1} \tag{16}$$

Hence, [*N*], the shape functions can be written as

$$[N]_{m\times 2m} = [A_c]_{m\times 2m} [A_e]^{-1}{}_{2m\times 2m} \tag{17}$$

For element with 10 degrees of freedom per node (m=10), *[N]* can be derived as shown below.

$$[\mathrm{N}]= \begin{bmatrix} N^t_{3\times 3} & 0_{3\times 3} & N^\tau_{3\times 4} & N^t_{3\times 3} & 0_{3\times 3} & N^\tau_{3\times 4} \\ 0_{3\times 3} & N^b_{3\times 3} & N^\tau_{3\times 4} & 0_{3\times 3} & N^b_{3\times 3} & N^\tau_{3\times 4} \\ 0_{4\times 3} & 0_{4\times 3} & N^\tau_{4\times 4} & 0_{4\times 3} & 0_{4\times 3} & N^\tau_{4\times 4} \end{bmatrix} \tag{18}$$

where $[N^\tau]$ are the shape functions corresponding to the shear stresses τ^t_{xz}, τ^b_{xz} and transverse normal stresses, σ^t_{zz} and σ^b_{zz}. The strain displacement relationship is given by

$$\{\epsilon\} = [\,B_s\,]\ \ \{\,u^e\,\} \tag{19}$$

where $[B\_s]$ is the strain displacement matrix. The above relation can be explicitly written as

$$\{\epsilon_i\} = [\,B_i\,]\ \ \{\,u^e\,\} \tag{20}$$

where subscript i in above equation refers to t, b and c corresponding to top face sheet, bottom face sheet and core respectively. $[B_t], [B_c]$ and $[B_b]$ are determined using the strain displacement relations as shown below.

$$\begin{aligned}\{\epsilon_t\} &= \begin{Bmatrix} \epsilon^t_{xx} \\ \gamma^t_{xz} \end{Bmatrix} = \begin{Bmatrix} \dfrac{\partial u_t}{\partial x} \\ \dfrac{\partial u_t}{\partial z_t} + \dfrac{\partial w_t}{\partial x} \end{Bmatrix} \\ &= \begin{Bmatrix} \dfrac{\partial N_1}{\partial x} - z_t \dfrac{\partial N_3}{\partial x} \\ -N_3 + \dfrac{\partial N_2}{\partial x} \end{Bmatrix} \{\,u^e\,\} = [\,B_t\,]\ \ \{\,u^e\,\}\ \ ]\end{aligned} \tag{21}$$

$$\{\epsilon_b\} = \begin{Bmatrix} \epsilon^b_{xx} \\ \gamma^b_{xz} \end{Bmatrix} = \begin{Bmatrix} \dfrac{\partial u_b}{\partial x} \\ \dfrac{\partial u_b}{\partial z_b} + \dfrac{\partial w_b}{\partial x} \end{Bmatrix}$$

$$= \begin{Bmatrix} \dfrac{\partial N_4}{\partial x} - z_t \dfrac{\partial N_6}{\partial x} \\ -N_6 + \dfrac{\partial N_5}{\partial x} \end{Bmatrix} \{\,u^e\,\} = [\,B_b\,]\ \ \{\,u^e\,\}$$

Assuming the displacements in longitudinal and transverse directions, u_c and w_c, as linear variation of corresponding displacements at core face sheet interfaces at both top and bottom, strain in core can be written as

$$\{\epsilon_c\} = \begin{Bmatrix} \epsilon_{xx}^c \\ \epsilon_{zz}^c \\ \gamma_{xz}^c \end{Bmatrix} = \begin{Bmatrix} \dfrac{\partial u_c}{\partial x} \\ \dfrac{\partial w_c}{\partial z} \\ \dfrac{\partial u_c}{\partial z_c} + \dfrac{\partial w_c}{\partial x} \end{Bmatrix} = [B_c]\{u^e\} \tag{23}$$

Where

$$[B_c] = \begin{Bmatrix} \left(\dfrac{\partial N_1}{\partial x} + \dfrac{h_t}{2}\dfrac{\partial N_3}{\partial x}\right) hc_1 + \left(\dfrac{\partial N_4}{\partial x} - \dfrac{h_b}{2}\dfrac{\partial N_6}{\partial x}\right) hc_2 \\ \dfrac{1}{h_c}[N_2 - N_5] \\ \dfrac{1}{h_c}[N_h] + hc_1 \dfrac{\partial N_2}{\partial x} + hc_2 \dfrac{\partial N_5}{\partial x} \end{Bmatrix}$$

And N_h is defined as $[N_1 - N_4 + \frac{h_t}{2}N_3 + \frac{h_b}{2}N_6]$, where N_1, N_2, N_3, N_4, N_5 and N_6 are the shape functions corresponds to $u_{0t}, w_t, \frac{\partial w_t}{\partial x}, u_{0b}, w_b, \frac{\partial w_b}{\partial x}$ respectively. In Eqn 18, N^t represents N_1, N_2 and N_3, while N^b represents N_4, N_5 and N_6. Also $hc_1 = [\frac{1}{2} + \frac{z_c}{h_c}]$ and $hc_2 = [\frac{1}{2} - \frac{z_c}{h_c}]$ where z_c is the ordinate distance from the mid core section. The total stiffness matrix of the element is given by

$$[K^e] = [K_i] + [K_b] + [K_c] \tag{24}$$

where $[K^e]$ is the element stiffness matrix of beam which is obtained by integrating the stiffness contributions from top face $[K_t]$, bottom face, $[K_b]$ and core, $[K_c]$.
Where

$$[K_t]_{2m\times 2m} = b\int_0^L \int_{-\frac{h_t}{2}}^{\frac{h_t}{2}} [B_i]^T [Q_t][B_t] dz_t dx$$

$$[K_b]_{2m\times 2m} = b\int_0^L \int_{-\frac{h_b}{2}}^{\frac{h_b}{2}} [B_b]^T [Q_b][B_b] dz_b dx \tag{25}$$

$$[K_c]_{2m\times 2m} = b\int_0^L \int_{-\frac{h_c}{2}}^{\frac{h_c}{2}} [B_c]^T [Q_c][B_c] dz_c dx$$

In the above equation, [B] and [Q] matrices are represented with subscripts t, b, c corresponding to the top, bottom face sheets and core. h_t, h_b, h_c, z_t, z_b and z_c are the thickness of face sheets, core and corresponding ordinates. Forces acting on the element at the nodes are written as

$$\{F\} = \begin{Bmatrix} N_{x1}^t, \mathrm{V}_1^t, M_1^t, N_{x1}^b, \mathrm{V}_1^b, M_1^b, \\ N_{x2}^t, \mathrm{V}_2^t, M_2^t, N_{x2}^b, \mathrm{V}_2^b, M_2^b \end{Bmatrix}^T \tag{26}$$

It can be observed that the forces considered are 6 per node only which are related to the face sheets only. The forces corresponding to τ_{xz}, σ_{zz} are acting internally at the face sheet interfaces and hence the stiffness terms can be condensed out to get the effective stiffness matrix in terms of 6 dof per node, with an element stiffness matrix of size 12×12.

2.3 Mass matrix

Consistent mass matrix for top and bottom face sheets can be computed using the interpolation or shape functions that are used to derive the stiffness, as given by the following expression.

$$[M_t^c]_{2m\times 2m} = b\int_0^L \int_{-\frac{h_t}{2}}^{\frac{h_t}{2}} [N]^T [\rho_t][N] dz_t dx \tag{27}$$

$$[M_b^c]_{2m\times 2m} = b\int_0^L \int_{-\frac{h_b}{2}}^{\frac{h_b}{2}} [N]^T [\rho_b][N] dz_b dx \tag{28}$$

where $[M_t^c]$ and $[M_b^c]$ are the consistent mass matrices corresponding to the top and bottom face sheets. Since the degrees of freedom from core u_c, w_c are not considered and the shape functions are not represented for core, the mass of the core cannot be computed using consistent mass matrix. However, the mass can be lumped at the respective degree of freedom corresponding to the degrees of freedom represented at top and bottom face sheets.

Lumped mass matrix is a diagonal matrix, which is obtained by placing particle masses at nodes (Cook *et al.* 2002). Total element mass of the core, $m_c = \rho_c A_c L$, where A_c is the cross-sectional area of core. Particle lumping places a particle of mass $\frac{\mathrm{m_c}}{4}$ at each translational-longitudinal and transverse degree of freedom. Rotational inertia can be calculated as $\frac{1}{3}\frac{\mathrm{m_c}}{4}\left(\frac{L}{2}\right)^2 = \frac{\mathrm{m_c}}{48}L^2$. Mass corresponding to the shear stress terms are taken as zeros.

In consistent mass model, the consistent mass matrices from face sheets are computed using the interpolation functions used for stiffness and the lumped mass matrix from core is added as shown below.

$$[M_c^e] = [M_t^c] + [M_b^c] + [M_c] \tag{29}$$

Here the elements of diagonal mass matrix for core $[M_c]$ for a standard element with 6 dof per node is given by

$$\{M_l^c\} = \frac{\rho_c A_c L}{4}\left\{1,1,\frac{1}{12},1,1,\frac{1}{12},1,1,\frac{1}{12},1,1,\frac{1}{12}\right\}^T \tag{30}$$

In case of an element with stress degrees of freedom, the corresponding elements in mass matrix considered are zeros. In lumped mass model, the mass matrices from face sheets are computed using the lumped model and the lumped mass matrix from core is added as shown below.

$$[M_l^e] = [M_t^l] + [M_b^l] + [M_c] \tag{31}$$

Mass matrix from core, M_c will be same as shown above in Eq. (30). The lumped mass matrices for face sheets M_t^l and M_b^l are computed in similar manner and are defined as shown below.

$$\{M_t^l\} = \frac{\rho_t A_t L}{2}\left\{1,1,\frac{1}{12},1,1,\frac{1}{12},1,1,\frac{1}{12},1,1,\frac{1}{12}\right\}^T \tag{32}$$

$$\{M_b^l\} = \frac{\rho_b A_b L}{2}\left\{1{,}1,\frac{1}{12},1{,}1,\frac{1}{12},1{,}1,\frac{1}{12},1{,}1,\frac{1}{12}\right\}^T \quad (33)$$

In this paper, wherever consistent mass model is referred to, then it means that the matrices are computed using Eqn.29 and while the lumped mass model refers to the mass computed using Eq. (31).

2.4 Global matrices and their solution

Once elemental stiffness, mass and force matrices are derived, then these matrices need to be assembled based on the discretisation carried out to model the given structure for analysis. Assembly of these matrices is done according to the nodes connected to define an element and global equation number assigned to the degrees of freedom at nodes n_i and n_j, where n_i and n_j are the first and second nodes of the element. The numbering is done taking the boundary conditions defined at some nodes. Assembly of these matrices will give global stiffness$[K]$, global mass $[M]$ and global force vector $\{F\}$ which are having the dimensions of number of equations present in the system.

The dynamic equations of motion can be written as follows.

$$[M]_{nq\times nq}\{\ddot{u}\}_{nq\times 1} + [K]_{nq\times nq}\{u\}_{nq\times 1} = \{F\}_{nq\times 1} \quad (34)$$

where nq is the number of equations or unknown in the system to be solved. This is an equation which is defining the undamped dynamic system when the force applied is time dependant. The above equation can be solved using Newton- β time stepping algorithm, the details of which is given in standard text books Cook *et al*. (2002), Shames and Clive (2003).

3. Four DOF rigid core euler bernoulli beam element (Eul4d)

This is sandwich beam model with incompressible core and symmetric face sheets having equal thickness, where the transverse displacements are assumed same in both top and bottom face sheets, meaning $w_t = w_b = w$. The nodal degrees of freedom are $u_{0t}, w, \frac{\partial w}{\partial x}, u_{0b}$. As the face sheets are having same thickness, the stiffness coefficients $A_t = A_b = A$, $A_{11t} = A_{11b} = A_{11}$, $B_{11t} = B_{11b} = 0$ and $D_{11t} = D_{11b} = D_{11}$.

In this idealization, as the transverse displacement in top and bottom face sheets is assumed the same, which will be the case applicable for thin cores. This results in zero normal stress in transverse direction, i.e., $\sigma_{zz} = 0$. This result comes from the core equilibrium equations, that is $\frac{\partial \tau_{xz}}{\partial x} = 0$

Assuming Euler Bernoulli beam theory for face sheets in the present idealization, the following kinematics of deformation is applicable.

$$u_t(x,z,t) = u_{0t}(x,t) - z_t \frac{dw(x,t)}{dx}$$
$$w_t(x,z,t) = w_b(x,z,t) = w(x,t) \quad (35)$$
$$\phi_t(x,z,t) = \phi_b(x,z,t) = \frac{\partial w}{\partial x}$$
$$u_b(x,z,t) = u_{0b}(x,t) + z_b \frac{dw(x,t)}{dx}$$

In this model, the face sheets are considered having equal thickness $h_t = h_b = h$ and hence, it gives the same geometrical sectional properties and similarly, $I_{0t} = I_{0b} = I_0$, $I_{1t} = I_{1b} = 0$. It is assumed that the energy transfer between face sheets and core at interfaces is through shear stress from the core, τ_{xz}^c only.

Following governing equations are obtained by considering the equal thickness face sheets.

$$I_0\frac{\partial^2 u_{0t}}{\partial t^2} - b A_{11}\frac{\partial^2 u_{0t}}{\partial x^2} - b\,\tau_{xz}^t = 0 \quad (36)$$

$$I_0\frac{\partial^2 w}{\partial t^2} - b D_{11}\frac{\partial^4 w}{\partial x^4} + b\frac{h}{2}\frac{\partial \tau_{xz}^t}{\partial x} = 0 \quad (37)$$

$$I_0\frac{\partial^2 u_{0b}}{\partial t^2} - b A_{11}\frac{\partial^2 u_{0b}}{\partial x^2} + b\,\tau_{xz}^b = 0 \quad (38)$$

$$I_0\frac{\partial^2 w}{\partial t^2} - b D_{11}\frac{\partial^4 w}{\partial x^4} + b\frac{h}{2}\frac{\partial \tau_{xz}^b}{\partial x} = 0 \quad (39)$$

Eq. (39) is same as Eq. (37) since τ^t is equal to τ^b. Associated force boundary conditions are as given below.

$$\begin{aligned} b A_{11}\frac{\partial u_{0t}}{\partial x} &= N^t \\ b D_{11}\frac{\partial^2 w}{\partial x^2} &= M^t \\ -b D_{11}\frac{\partial^3 w}{\partial x^3} + b\frac{h_t}{2}\tau_{xz}^t &= V^t \\ b A_{11}\frac{\partial u_{0b}}{\partial x} &= N\text{^}b \end{aligned} \quad (40)$$

Without considering the inertial term, Eqs. (36)-(39) can be written as

$$-b A_{11}\frac{\partial^2 u_{0t}}{\partial x^2} - b\,\tau_{xz}^t = 0 \quad (41)$$

$$-b D_{11}\frac{\partial^4 w}{\partial x^4} + b\frac{h}{2}\frac{\partial \tau_{xz}^t}{\partial x} = 0 \quad (42)$$

$$-b A_{11}\frac{\partial^2 u_{0b}}{\partial x^2} + b\,\tau_{xz}^b = 0 \quad (43)$$

Core is assumed to be incompressible in transverse direction and hence $\sigma_{zz}^c = 0$ prevails and the interaction between face sheets in overall sandwich beam behaviour is through shear stress. The equilibrium equations for core will become,

$$\frac{\partial \sigma_{xx}^c}{\partial x} + \frac{\partial \tau_{xz}^c}{\partial z} = 0 \quad (44)$$

$$\frac{\partial \tau_{xz}^t}{\partial x} = 0 \quad (45)$$

Which means that the shear stress is constant along X axis. Referring to Eq. (42), as τ_{xz}^{c} is constant in x, this will force $\frac{\partial^4 w}{\partial x^4}$ =0. Hence, the polynomial order of w can be 3^{rd} order. Accordingly, u_{0t} and u_{0b} will be quadratic. From the constitutive relation, τ_{xz}^{c} can be written as

$$\tau_{xz}^{c} = \frac{\partial u_c}{\partial z} + \frac{\partial w}{\partial x} \tag{46}$$

If longitudinal displacement in core, u_c is assumed to vary linearly between longitudinal displacements at interfaces u_t and u_b, it results in a constant value of $\frac{\partial u_c}{\partial z}$ across the core. As $\frac{\partial w}{\partial x}$ is constant across the depth of core, this will enforce $\tau_{xz}^{t} = \tau_{xz}^{b}$, thereby $\frac{\partial^2 u_c}{\partial x^2}$ =0.For bending to be present in the core of beam, $u_c$should vary at least as quadratic function in z_c across the depth of core. As the core is assumed to be rigid, the bending contribution from core is negligible and hence, $\frac{\partial^2 u_c}{\partial x^2}$ =0 and $u_c$will vary linearly across the depth of core. From Eq. (46), u_c can be written as

$$\frac{\partial u_c}{\partial z} = \frac{\tau_{xz}^{c}}{G_c} - \frac{\partial w}{\partial x} \tag{47}$$

On integration with respect to z, u_c can be determined as,

$$u_c = u_{0t} + (\frac{h_t}{2} + \frac{h_c}{2} - z_c)\frac{dw}{dx} + (z_c - \frac{h_c}{2})\frac{\tau_{xz}^{c}}{G_c} \tag{48}$$

Using the expression for u_c, σ_{xx}^{c} can be written as,

$$\frac{\partial \sigma_{xx}^{c}}{\partial x} = E_C \frac{\partial^2 u_{0t}}{\partial x^2} + E_c(\frac{h_t}{2} + \frac{h_c}{2} - z_c)\frac{d^3 w}{dx^3} = 0 \tag{49}$$

From Eq. (44) upon integration, one ca =n write,

$$\tau_{xz}^{t} - \tau_{xz}^{b} + E_c h_c \frac{\partial^2 u_{0t}}{\partial x^2} + E_c h_c \left(\frac{h_t + h_c}{2}\right)\frac{d^3 w}{dx^3} = 0 \tag{50}$$

As $\tau_{xz}^{t} = \tau_{xz}^{b}$, the above equation will be reduced to,

$$E_c h_c \frac{\partial^2 u_{0t}}{\partial x^2} + E_c h_c \left(\frac{h_t + h_c}{2}\right)\frac{d^3 w}{dx^3} = 0 \tag{51}$$

From Eqs. (41) and (43), as $\tau^{t} = \tau^{b}$, we can derive a relation between u_{0t} and u_{0b} as,

$$\frac{\partial^2 u_{0t}}{\partial x^2} = -\frac{\partial^2 u_{0b}}{\partial x^2} \tag{52}$$

Based on the above observations and relations, the displacement fields can be assumed as

$$\begin{aligned} u_{0t} &= a_0 + a_1 x + a_2 x^2 \\ u_{0b} &= a_3 + a_4 x - a_2 x^2 \\ w &= a_5 + a_6 x + a_7 x^2 + a_8 x^3 \\ \frac{\partial w}{\partial x} &= a_6 + 2\, a_7 x + 3\, a_8 x^2 = \theta \end{aligned} \tag{53}$$

Total number of unknown polynomial coefficients are 9 and N_x^t, V_x, M_x, N_x^b are forces at node, which makes to 8 force resultants per element. One more unknown polynomial coefficient needs to be determined so that the total number of unknown polynomial coefficients will become 8 to define the displacement functions completely. We can use Eq. (52) to get this additional condition, which is given by, $a_8 = c_1 a_2$, where $c_1 = \frac{2}{3(h_t + h_c)}$.Accordingly, the polynomials expressed in Eq. (53) can be rewritten as,

$$\begin{aligned} u_{0t} &= a_0 + a_1 x + a_2 x^2 \\ u_{0b} &= a_3 + a_4 x - a_2 x^2 \\ w &= a_5 + a_6 x + a_7 x^2 + c_1 a_2 x^3 \\ \frac{\partial w}{\partial x} &= a_6 + 2\, a_7 x + 3\, c_1 a_2 x^2 = \theta \end{aligned} \tag{54}$$

In this element, the shear stress from core is constant across the interface of the core and also the rotation is the derived quantity from the transverse displacement, which ensures that the shear locking will not occur. In this formulation, expressions given in Eq. (54) are considered as interpolating functions corresponding to the degrees of freedom of element, $\{u\}^T = \{u_{0t}, w, \frac{\partial w}{\partial x}, u_{0b}\}$. Using the procedure explained in Eqs. (14) to (17), the displacement functions can be expressed in terms of nodal displacements, $\{u_e\}^T$ at both ends of element, x=0 and x=L through shape function of element, $[N]^T$ as shown below.

$$\{u\}_{4\times 1} = [N]_{4\times 8}\, \{u^e\}_{8\times 1} \tag{55}$$

In this element, the strains considered in face sheets are ϵ_{xx} only while the strains in core are ϵ_{xx}^{c}, γ_{xz}^{c}. The stiffness matrix of element is determined and is given by

$$[K^e]_{8\times 8} = [K_t] + [K_b] + [K_c] \tag{56}$$

where $[K^e]$ is the element stiffness matrix of beam obtained by integrating the stiffness contributions from top face $[K_t]$, bottom face, $[K_b]$ and core, $[K_c]$. Forces acting on the element at the nodes are written as

$$\{F\}^T = \{N_1^t, V_1^t, M_1^t, N_1^b, N_2^t, V_2^t, M_2^t, N_2^b\} \tag{57}$$

Once the stiffness and force matrices are obtained at element level, assembly of these for all elements discretized to model the given structure is done to get the global or overall system matrices. These matrices are solved to find out the unknowns.

Mass matrix of element is built with contributions from face sheets and core, as given by

$$[M^e] = [M_t] + [M_b] + [M_c] \tag{58}$$

Mass matrices from top and bottom face sheets are computed using the consistent mass model using the shape functions derived above in Eq. (54). $[M_t]$ and $[M_b]$ are computed as given in Eqs. (27) and (28). As the displacements from core u_c, w_c are not available as degrees of freedom, the mass from core is lumped at the corresponding degrees of freedom that belongs to face sheet. Lumped mass matrix from core for the present element is given by,

$$\{M_c\}^T = \frac{\rho_c A_c L}{4}\{1,2,\frac{L}{6},1,1,2,\frac{L}{6},1\}$$

4. Ten DOF flexible core euler bernoulli beam element (Eul10d)

This is higher order element assuming the flexible effects of core by considering the presence of both shear stress and normal transverse stresses along with the six displacement dof which are independent at both the top and bottom face sheets. Free body diagram, of and forces details are shown earlier in Figs. 1 and 2. Applying Hamilton's principle for the top and bottom face sheets, the following governing differential equations are obtained.

For top face sheets, the governing equations are given by

$$I_{0t}\,\frac{\partial^2 u_{0t}}{\partial t^2} - I_{it}\,\frac{\partial^3 w_t}{\partial t^2\,\partial x} - b\,A_{11t}\,\frac{\partial^2 u_{0t}}{\partial x^2} + b\,B_{11t}\,\frac{\partial^3 w_t}{\partial x^3} - b\tau_{xz}^t = 0 \tag{59}$$

$$\begin{aligned} I_{0t}\,\frac{\partial^2 w_t}{\partial t^2} - I_{it}\,\frac{\partial^2 u_{0t}}{\partial t^2} + b\,B_{11t}\,\frac{\partial^3 u_{0t}}{\partial x^3} \\ -b\,D_{11t}\,\frac{\partial^4 w_t}{\partial x^4} - b\sigma_{zz}^t + b\frac{h_t}{2}\,\frac{\partial \tau_{xz}^t}{\partial x} = 0 \end{aligned} \tag{60}$$

For bottom face sheets, the same can be written as

$$\begin{aligned} I_{0b}\,\frac{\partial^2 u_{0b}}{\partial t^2} - I_{ib}\,\frac{\partial^3 w_b}{\partial t^2\,\partial x} - b\,A_{11b}\,\frac{\partial^2 u_{0b}}{\partial x^2} \\ + b\,B_{11b}\,\frac{\partial^3 w_b}{\partial x^3} + b\tau_{xz}^b = 0 \end{aligned} \tag{61}$$

$$\begin{aligned} I_{0b}\,\frac{\partial^2 w_b}{\partial t^2} - I_{it}\,\frac{\partial^2 u_{0b}}{\partial t^2} + b\,B_{11b}\,\frac{\partial^3 u_{0b}}{\partial x^3} \\ -b\,D_{11b}\,\frac{\partial^4 w_b}{\partial x^4} + b\sigma_{zz}^b + b\frac{h_b}{2}\,\frac{\partial \tau_{xz}^b}{\partial x} = 0 \end{aligned} \tag{62}$$

The associated forced boundary conditions for top and bottom sheets can be expressed as given below.

$$\begin{aligned} b\,A_{11t}\,\frac{\partial u_{0t}}{\partial x} - b\,B_{11t}\,\frac{\partial^2 w_t}{\partial x^2} &= N^t \\ b\,B_{11t}\,\frac{\partial u_{0t}}{\partial x} - b\,D_{11t}\,\frac{\partial^2 w_t}{\partial x^2} &= M^t \\ b\,B_{11t}\,\frac{\partial^2 u_{0t}}{\partial x^2} - b\,D_{11t}\,\frac{\partial^3 w_t}{\partial x^3} + b\frac{h_t}{2}\tau_{xz}^t &= V^t \\ b\,A_{11b}\,\frac{\partial u_{0b}}{\partial x} - b\,B_{11b}\,\frac{\partial^2 w_b}{\partial x^2} &= N^b \\ b\,B_{11b}\,\frac{\partial u_{0b}}{\partial x} - b\,D_{11b}\,\frac{\partial^2 w_b}{\partial x^2} &= M^b \\ b\,B_{11b}\,\frac{\partial^2 u_{0b}}{\partial x^2} - b\,D_{11b}\,\frac{\partial^3 w_b}{\partial x^3} + b\frac{h_t}{2}\tau_{xz}^b &= V^b \end{aligned} \tag{63}$$

where as N^t, V^t, M^t, N^b, V^b and M^b represents the axial force, shear force and bending moment acting at two ends of beam, acting at top and bottom face sheets. It is to be noted that the governing equations derived above are corresponding to the top and bottom face sheets of the sandwich beam, wherein the effect of core has been included through the shear stress of the core τ_{xz}^c and the transverse normal stress σ_{zz}^c. In order to proceed with the super convergent formulation, we need to obtain exact solution to Eqs. (59)-(62). As the number of degrees of freedom considered in the element are 10, total number of degrees of freedom and force resultants available in the element at two nodes is equal to 20. Here we need to follow certain approach to determine the order of polynomials of different dof.

It can be observed that the degree of freedom with minimum polynomial order is for variables σ_{zz}^t and σ_{zz}^b. Assuming the constant variation for σ_{zz}^t and σ_{zz}^b, corresponding polynomial orders for other degrees of freedom τ_{xz}^t, τ_{xz}^b is linear, while $u_{0t}, u_{0b}, \phi_t, \phi_b$ is 3^{rd} order and w_t, w_b is 4^{th} order. This makes total number of polynomial unknown coefficients as 24. With these assumed polynomials order, the conditions from the Eqs. (59)-(62) that will result are about 6, which will yield about 18 unknown polynomial coefficients, lesser than the total number of degrees of freedom per element. Hence, the assumptions will not yield the exact interpolation functions. Assuming the linear variation for σ_{zz}^t and σ_{zz}^b, the total number of polynomial unknown coefficients will be 32 and the conditions that will result will be about 10 and this will yield about 22 unknown polynomial coefficients, more than the total number of degrees of freedom per element, which is equal to 20. In order to derive the exact interpolation functions, we need one more condition which will provide two relations between the polynomial coefficients. We can derive one more condition from core equilibrium equations as given below.

The governing core equations are given by

$$\frac{\partial \sigma_{xx}^c}{\partial x} + \frac{\partial \tau_{xz}^c}{\partial z} = 0 \tag{64}$$

$$\frac{\partial \sigma_{zz}^c}{\partial z} + \frac{\partial \tau_{xz}^c}{\partial x} = 0 \tag{65}$$

Assuming τ_{xz}^c as the linear variation across depth of core, between τ_{xz}^t and τ_{xz}^b, σ_{zz}^c can be computed as,

$$\tau_{xz}^c = \left(\frac{1}{2} + \frac{z_c}{h_c}\right)\tau_{xz}^t + \left(\frac{1}{2} - \frac{z_c}{h_c}\right)\tau_{xz}^b \tag{66}$$

$$\sigma_{zz}^c = -z_c \int \frac{\partial \tau_{xz}^c}{\partial x}\,\mathrm{dz} \tag{67}$$

σ_{zz}^c can be derived and σ_{zz}^b can be obtained as

$$\begin{aligned} \sigma_{zz}^c = \sigma_{zz}^t + \left(\frac{3\,h_c}{8} - \frac{z_c}{2} - \frac{z_c^2}{2\,h_c}\right)\frac{\partial\,\tau_{xz}^t}{\partial\,x} \\ + \left(\frac{3\,h_c}{8} - \frac{z_c}{2} + \frac{z_c^2}{2\,h_c}\right)\frac{\partial\,\tau_{xz}^b}{\partial\,x} \end{aligned} \tag{68}$$

$$\sigma_{zz}^b = \sigma_{zz}^t + \frac{h_c}{2}\left(\frac{\partial \tau_{xz}^t}{\partial x} + \frac{\partial \tau_{xz}^b}{\partial x}\right) \tag{69}$$

Eq. (69) can be rewritten as,

$$\sigma_{zz}^t - \sigma_{zz}^b + \frac{h_c}{2}\left(\frac{\partial \tau_{xz}^t}{\partial x} + \frac{\partial \tau_{xz}^b}{\partial x}\right) = 0 \tag{70}$$

If σ_{zz}^c assumes linear variation across longitudinal axis x of beam, Eq. (70) will provide two more conditions, which makes the total number of conditions as 12. This will make total number of unknown polynomial coefficients as 20. This will give the super convergence property as this will solve the governing equations exactly.

Assumed displacement fields are

$$\begin{aligned} u_{0t} &= a_0 + a_1\,x + a_2\,x^2 + a_3\,x^3 + a_4\,x^4 \\ w_t &= a_5 + a_6\,x + a_7\,x^2 + a_8\,x^3 + a_9\,x^4 + a_{10}\,x^5 \end{aligned} \tag{71}$$

$$\frac{\partial w_t}{\partial x} = a_6 + 2\,a_7 x + 3\,a_8 x^2 + 4\,a_9 x^3 + 5\,a_{10}\,x^4$$
$$\tau_{xz}^t = a_{11} + a_{12}\,x + a_{13}\,x^2$$
$$\sigma_{zz}^t = a_{14} + a_{15}\,x$$
$$u_{0b} = a_{16} + a_{17}\,x + a_{18}\,x^2 + a_{19}\,x^3 + a_{20}\,x^4$$
$$w_b = a_{21} + a_{22}x + a_{23}\,x^2 + a_{24}\,x^3 + a_{25}x^4 + a_{26}\,x^5$$
$$\frac{\partial w_b}{\partial x} = a_{22} + 2a_{23}x + 3\,a_{24}x^2 + 4\,a_{25}x^3 + 5a_{26}x^4$$
$$\tau_{xz}^b = a_{27} + a_{28}\,x + a_{29}\,x^2$$
$$\sigma_{zz}^b = a_{30} + a_{31}\,x$$

By substituting these polynomials in the governing equations, listed in Eqs. (59)-(62) and also additional equation from core Eq. (70), 12 conditions are obtained. From these conditions, some of the polynomial unknown coefficients are expressed in terms of other coefficients which will reduce the total number of unknown coefficients to 20. The displacement functions thus obtained by solving these equations are given as below.

$$\begin{aligned}
u_{0t} &= a_0 + a_1\,x + a_2\,x^2 + a_3\,x^3 + a_4\,x^4 \\
w_t &= d_2\,x^4\,a_3 + a_5 + x\,a_6 + a_7\,x^2 + a_8\,x^3 \\
&\quad + a_{10}\,x^5 + d_1\,x^4\,a_{19} + d_3\,x^4\,a_{25} \\
\frac{\partial w_t}{\partial x} &= 4\,x^3\,d_2\,a_3 + a_6 + 2\,x\,a_7 + 3\,x^2\,a_8 \\
&\quad + 5\,x^4\,a_{10} + 4\,x^3\,d_1\,a_{19} \\
&\quad + 4x^3 d_3\,a_{25} \\
\tau_{xz}^t &= -2A_{11t}a_2 + (24\,B_{11t}\,d_2 - 6\,A_{11t})xa_3 \\
&\quad - 12\,x^2 A_{11t}\,a_4 + 6B_{11t}a_8 \\
&\quad + 60\,x^2\,B_{11t}\,a_{10} + 24\,x\,B_{11t}\,d_1 a_{19} \\
&\quad + 24\,xB_{11t}d_3\,a_{25} \\
\sigma_{zz}^t &= d_{10}\,a_3 + (24\,B_{11t} - 12\,h_t\,A_{11t})x\,a_4 \\
&\quad + (60\,h_t\,B_{11t} - 120\,D_{11t})x\,a_{10} \\
&\quad + d_{11}a_{19} + d_{12}\,a_{25} \\
u_{0b} &= a_{16} + a_{17}\,x + a_{18}\,x^2 + a_{19}\,x^3 + a_{20}\,x^4 \\
w_b &= d_4\,x^5\,a_4 - d_5\,x^5\,a_{10} - d_6\,x^5\,a_20 + a_{21} \\
&\quad + a_{22}\,x + a_{23}x^2 + a_{24}\,x^3 + a_{25}\,x^4 \\
\frac{\partial w_b}{\partial x} &= 5x^4\,d_4\,a_4 - 5\,x^4\,d_5\,a_{10} - 5\,x^4\,d_6\,a_{20} + a_{22} \\
&\quad + 2\,x\,a_{23} + 3\,x^2\,a_{24} + 4\,x^3 a_{25} \\
\tau_{xz}^b &= -60\,d_4\,B_{11b}\,x^2\,a_4 + 60\,d_5\,B_{11b}x^2\,a_{10} \\
&\quad + 2\,A_{11b}\,a_{18} + 6\,x\,A_{11b}\,a_{19} \\
&\quad + (12\,A_{11b} + 60\,d_b\,B_{11b})x^2 a_{20} \\
&\quad - 6\,B_{11b}a_{24} - 24\,x\,B_{11b}\,a_{25} \\
\sigma_{zz}^b &= d_{13}\,x\,a_4 - d_{14}\,x\,a_{10} \\
&\quad - (6\,B_{11b} + 3\,h_b A_{11b})a_{19} \\
&\quad - d_{15}\,x\,a_{20} \\
&\quad + (24\,D_{11b} + 12\,h_b B_{11b})a_{25}
\end{aligned} \tag{72}$$

Where

$$\begin{aligned}
d_1 &= \frac{6\,B_{11b} + 3\,h_b\,A_{11b} - 3\,h_c\,A_{11b}}{den_1} \\
d_2 &= \frac{6\,B_{11t} - 3\,h_t\,A_{11t} + 3\,h_c\,A_{11t}}{den_1} \\
d_3 &= -\frac{24\,D_{11b} + 12\,h_b\,B_{11b} - 12\,h_c\,B_{11b}}{den_1} \\
d_4 &= \frac{24\,B_{11t} - 12\,(h_t - h_c)A_{11t}}{den_2} \\
d_5 &= \frac{12\,A_{11b}\,(h_c - h_b) - 24\,B_{11b}}{den_2} \\
d_6 &= \frac{60(h_c - h_t)B_{11t} + 120\,D_{11t}}{den_2} \\
d_7 &= (120\,D_{11b} + 60\,h_b\,B_{11b})d_4 \\
d_8 &= (120\,D_{11b} + 60\,h_b\,B_{11b})d_5 \\
d_9 &= 12h_b A_{11b} + B_{11b}(24 + 60\,h_b d_6) + 120\,D_{11b}\,d_6 \\
d_{10} &= 6\,B_{11t} - 3\,h_t A_{11t} + 12\,d_2\,B_{11t}\,h_t - 24\,d_2\,D_{11t} \\
d_{11} &= (12\,h_t B_{11t} - 24\,D_{11t})d_1 \\
d_{12} &= (12\,h_t\,B_{11t} - 24\,D_{11t})d_3 \\
d_{13} &= (120\,D_{11b} + 60\,h_b\,B_{11b})d_4 \\
d_{14} &= (120\,D_{11b} + 60\,h_b\,B_{11b})d_5 \\
d_{15} &= 24\,B_{11b} + 12\,h_b\,A_{11b} \\
&\quad + (120\,D_{11b} + 60\,h_b\,B_{11b})d_6 \\
den_1 &= 12\,B_{11t}\,h_c - 12\,B_{11t}\,h_t + 24\,D_{11t} \\
den_2 &= 120\,D_{11b} + 60\,(h_b - h_c)B_{11b}
\end{aligned} \tag{73}$$

It can be noted that a_0, a_1, a_2, a_3, a_4, a_5, a_6, a_7, a_8, a_{10}, a_{16}, a_{17}, a_{18}, a_{19}, a_{20}, a_{21}, a_{22}, a_{23}, a_{24}, a_{25} are independent unknown polynomial coefficients, which need to be evaluated. The expressions defined in Eq. (72) will be used as interpolating functions in super convergent element formulation while deriving the stiffness matrix of the element. Using the procedure explained in Eqs. (14)-(17), the displacement functions can be expressed in terms of nodal displacements, $\{u_e\}^T$ at both ends of element, $x = 0$ and $x = L$ through shape function of element, $[N]^T$ as shown below.

$$\{u\}_{10\times 1} = [N]_{10\times 20}\{u^e\}_{20\times 1} \tag{74}$$

In this element, the strains considered in face sheets are ϵ_{xx} only while the strains in core are ϵ_{xx}^c, ϵ_{zz}^c and γ_{xz}^c. As explained earlier, the stiffness matrix of element is determined and is given by

$$[K^e]_{20\times 20} = [K_t] + [K_b] + [K_c] \tag{75}$$

Where $[K^e]$ is the element stiffness matrix of beam obtained by integrating the stiffness contributions from top face $[K_t]$, bottom face, $[K_b]$ and core, $[K_c]$.

Forces acting on the element at the nodes are written as

$$\{F^e\} = \begin{Bmatrix} N_1^t, V_1^t, M_1^t, \tau_1^t, N_{z1}^t, N_1^b, V_1^b, M_1^b, \tau_1^b, N_{z1}^b \\ N_2^t, V_2^t, M_2^t, \tau_2^t, N_{z2}^t, N_{z2}^b, V_2^b, M_2^b, \tau_2^b, N_{z2}^b \end{Bmatrix}^T \tag{76}$$

Once the stiffness and force matrices are obtained at element level, assembly of these for all elements discretized to model the given structure is done to get the global or overall system matrices. These matrices are solved to find out the unknowns.

Mass matrix of element is built with contributions from face sheets and core, as given by

$$[M^e] = [M_t] + [M_b] + [M_c] \tag{77}$$

Mass matrices from top and bottom face sheets are computed using the consistent mass model using the shape functions derived above in Eq. (72). $[M_t]$ and $[M_b]$ are computed as given in Eqs. (27) and (28). As the displacements from core u_c, w_c are not available as degrees of freedom, the mass from core is lumped at the corresponding degrees of freedom that belongs to face sheet. Lumped mass matrix from core for the present element is given by,

$$\{M_c\} = \frac{\rho_c A_c L}{4} \begin{Bmatrix} 1,1,\frac{L}{12},0,0,1,1,\frac{L}{12},0,0, \\ 1,1,\frac{L}{12},0,0,1,1,\frac{L}{12},0,0 \end{Bmatrix}^T$$

The elements corresponding to shear and normal transverse stresses needs to be condensed out. The condensation process to obtain the reduced matrices is done by expressing the internal degrees of freedom in terms of degrees of freedom at boundaries. The reduced matrices for $[K_r]$, $[M_r]$ and $[F_r]$ can be expressed as,

$$[K_r]_{12\times12} = [T]^T_{12\times20}[K]_{20\times20}[T]_{20\times12} \tag{78}$$

$$[M_r]_{12\times12} = [T]^T_{12\times20}[M]_{20\times20}[T]_{20\times12} \tag{79}$$

$$[F_r]_{12\times12} = [T]^T_{12\times20}[F]_{20\times20}[T]_{20\times12} \tag{80}$$

where $[K]$ represents the overall stiffness matrix $[M]$ is the overall mass matrix and $[F]$ represents the force vector for overall system.

The dynamic equation of motion can be written as follows.

$$[M_r]\ \{\ddot{u}\} + [K_r]\{u\} = \{F_r\} \tag{81}$$

The solution of this equation is as explained earlier in subsection '*Global matrices and their solution*'.

5. Numerical experiments

The formulated element has super convergent property as explained in the earlier sections and so one element is sufficient to capture the exact response for static analysis, with concentrated loads, which results in substantial reduction in the system size. For dynamic analysis, for a given discretization, the accuracy of the present formulation is expected to be superior to elements formulated based on conventional polynomial approximation. This is because, the stiffness of the structure is exactly represented even though the inertial distribution is approximate. Hence, good accuracy in dynamic analysis can be expected from this element using smaller system sizes.

The aim of this section is twin fold, first is to validate the element with some of the available results from published literature and the second is to bring forth the super convergence property of the formulated element. These objectives are verified for a number of examples under static, free vibration and wave propagation analysis. Both metallic and composite face sheets are considered in the analysis. One example on wave propagation is presented to illustrate the computational advantages, accuracy of the results that can be obtained using the present element under high frequency impact.

5.1 Static analysis

Test cases are studied in this section in order to validate the formulated elements for static analysis under various load conditions such as point load, uniformly distributed load. The aim of these examples is to demonstrate the super convergence property and validation of these elements.

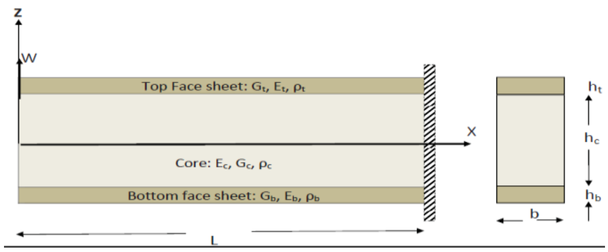

Fig. 3 Cantilever beam subjected to point load

Table 1 Sandwich beam details for static loads

Material properties	
Face sheets: Young's modulus (E_f) Mass density (ρ_f) Poisson's ratio (ν_f)	Aluminium 68970 N/mm^2, 2683 kg/m^3 , 0.3
Core: Shear modulus (G_c) Mass density(ρ_c) Poisson's ratio, (ν_c)	Calcium Alginate 82.764 N/ mm^2 32.8381 kg/m^3 0.3
Geometry Details	
Length 'l' and width 'b'of the beam	1000 mm, 40 mm,
Length to depth ratio 'l/H'	100
thickness ratio of core to face sheets,h_c/h	10
thickness ratio of face sheets, h_t/h_b	1
Load, at free end of top face sheet	Unit point load

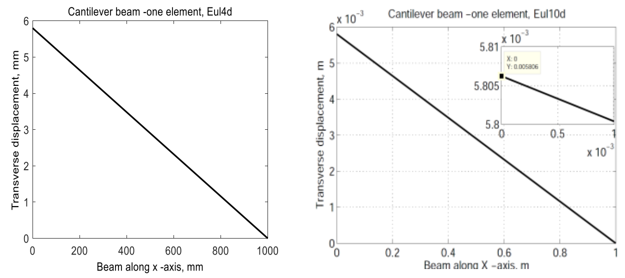

(a) Eul4d (b) Eul10d

Fig. 4 Transverse displacement profile of a cantilever beam with one element

5.1.1 Cantilever beam with metallic face sheet

A simple case of a cantilever beam (Fig. 3) subjected to a point load at the free end is considered to verify the displacement prediction with the developed elements. In the present case, the analysis is carried out for the beam configuration given as in above Table 1.

The transverse displacement profile along the length of beam is shown in Fig. 4. The value of displacements plotted at midpoint of core, which is computed as the average of the corresponding displacement of the top and bottom face sheets. The exact displacement as given by Backstrom and Nilson (2007) in case of cantilever sandwich beam at midpoint of the core is given as $\frac{WL^3}{3EI}+\frac{WL}{G_c bh_c}$, where EI is the section rigidity with E being the Young's modulus and I being the moment of Inertia of the beam. W is the point

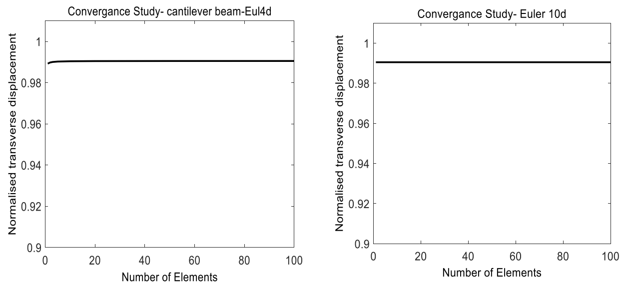

(a) Eul4d (b) Eul10d

Fig. 5 Super Convergence property of Euler elements

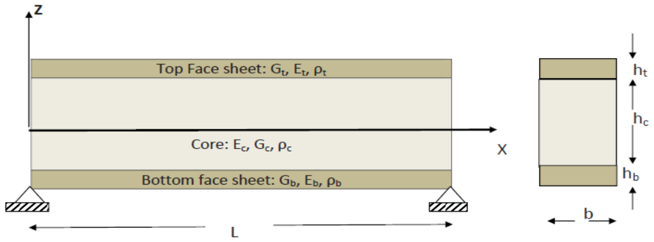

Fig. 6 Simply Supported beam

Table 2 Details of Sandwich beam with composite face sheets

Material properties	
Face sheets:	Glass Fiber
Modulus of Elasticity (E_t, E_b)	18000 MPa,
Poisson's ratio (ν_f)	0.3
Core:	Devincile foam
Modulus of Elasticity, E_c	140 MPa
Shear modulus, G_c	53.9 MPa
Geometry Details	
Length 'l' and width 'b' of the beam	1600 mm, 300 mm, 6
h_t, h_b, h_c	mm, 6 mm, 60 mm
Load, q_w	UDL of 0.10 Mpa

load which in this case is assumed as unity. By substituting the values appropriately given in Table 1, it can be found out that the transverse displacement turns out to be 5.8635 mm. It can be observed from the plots that the displacements obtained using one element matches well with the theoretical displacement value. Displacement profile clearly shows the top, bottom and mid core displacement values, which are zoomed in a window.

Fig. 4 shows the displacement profile captured with one element for element types Eul4d and Eul10d. For studying super convergence property of these elements, the number of elements are increased from 1 to 100 at regular intervals.

5.1.2 Super convergence

Super convergence property is examined next for a cantilever beam with $\frac{l}{H}$ ratio of 100 and h_c/h of 10 (h is the sum of the thicknesses of the top and bottom face sheets, ($h = h_t + h_b$) with a point load applied at free end on the top face sheet. The obtained displacements are normalized with exact solution obtained using the expression given by Backstrom and Nilson (2007). In case of element models with flexible core, the transverse displacement values at mid core are considered by averaging the displacements corresponding to the top and bottom face sheets. Normalized displacements for Eul4d and Eul10d element types with increasing number of elements are shown in Fig. 5.

It can be noticed that the normalized displacement values with one element for Euler Bernoulli beam elements Eul10d, Eul4d obtained are above 0.99 and these values are remaining constant with increase in number of elements. In other words, one element irrespective of the length of the element is sufficient to capture the displacement accurately for the case when the beam is loaded with point loads. Also, it is expected that all elements irrespective of whether the shear stress is constant or higher order across the longitudinal axis or across the depth of core, the formulated element will give accurate results. The displacements predicted are at top, bottom face sheets in case of Eul10d while the displacement predicted in case of Eul4d is at the center of core.

5.1.3 Simply supported beam with composite face sheets

In this case, we consider a simply supported beam with composite face sheet loaded under uniformly distributed loading (UDL) as shown in Fig. 6 and this problem have been reported by Frostig (2003). The beam parameters are given in Table 2.

In Eul4d, the transverse displacement degrees of freedom is constant though out the depth of element and hence the q_w UDL is theoretically applied at the center of core while practically it is not. In Eul10d element model, where the top and bottom transverse displacements are the degrees of freedom, acting at the face sheets, the loads are applied on the top face sheet.

Fig. 7(a) gives the displacement profile predicted by various theories and enlarged view of displacements where they are maximum are plotted in Fig. 7(b). From Fig. 7, it can be clearly observed that the present theory results are closely matching with other theories. Allen, Frostig using Ordinary Sandwich Panel Theory(OSPT) (Frostig (2003) predicts same displacements for both top and bottom face sheets. This is because, OSPT averages the displacement across the thickness coordinates. However, Higher order SAndwich Panel Theory(HSAPT) (Frostig 2003) predicts different top and bottom face sheets displacements. The displacements obtained using Eul10d element at top and bottom face sheets, which are represented in brackets with U for top face sheets and L for bottom face sheets are matching closely with other theories. This is because, HSAPT and the present theory interpolates the top and bottom displacements separately.

In case of higher order theories like HSAPT and Eul10d elements, the transverse displacements at top face sheets are allowed as free and hence the transverse displacements will not be zero at the supports unlike in other elements. The displacement values obtained at the supports can be clearly found from Fig. 7. Although the present formulation is exact in case with point loads, when the beam is subjected to uniformly distributed loading, it requires more elements to capture the behavior. While the displacements are

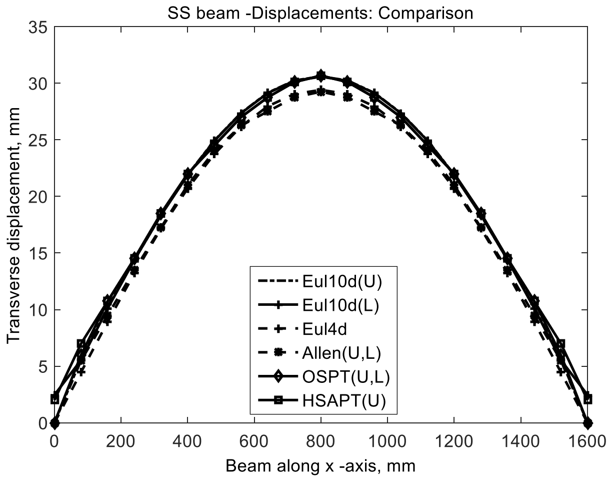

(a) Displacement profile

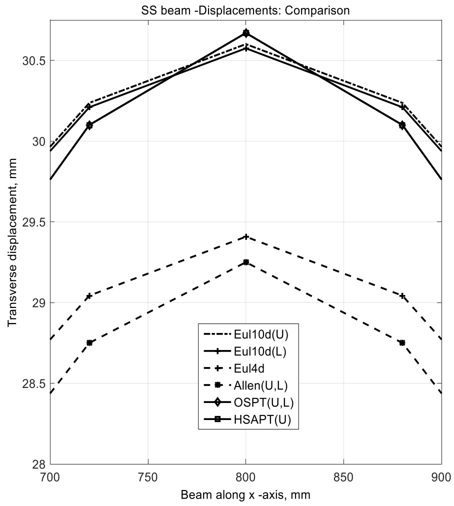

(b) Zoom at maximum location

Fig. 7 Displacement profile: SS Beam under UDL

Table 3 Details of Sandwich beam with metallic face sheets

Material properties	
Face sheets:	Aluminium
Young's modulus (E_f)	68970 N/mm^2,
Mass density (ρ_f)	2683 kg/m^3,
Poisson's ratio (ν_f)	0.3
Core:	Calcium Alginate
Shear modulus (G_c)	82.764 N/ mm^2
Mass density(ρ_c)	32.8381 kg/m^3
Poisson's ratio, (ν_c)	0.3
Geometry Details	
Length 'l' and width 'b' h_t, h_b, h_c	712.2 mm, 25.4 mm, 0.4572 mm, 0.4572 mm, 12.7 mm

accurately predicted even with less number of formulated elements, other theories require 20 elements and the values are obtained from the plots given in the work published by Frostig (2003).

It can be noticed that the models proposed with the rigid core where $w_t = w_b = w$, Eul4d predicts displacement as the average of displacements corresponding to top and bottom face sheets. These displacements are matching closely with the theories proposed by others such as Howard (1969). While the displacements predicted using Eul10d element at top and bottom face sheets, are matching well with OSPT and HSAPT Frostig (2003). Displacement values obtained using Eul4d, Eul10d and other theories are enlarged near the center of simply supported beam in Fig. 7(b) for study among various theories.

The displacements predicted by higher order element Eul10d are closely matching with the displacements obtained by OSPT and HSAPT theories. As expected, Eul4d values are matching with Allen and Eul10d values are matching well with OSPT, HSAPT higher order element theories.

Displacement profiles for the developed higher order elements using Euler Bernoulli beams-Eul10d were shown in Fig. 7(b). This is to see the variation of transverse displacements of top and bottom face sheets. In case of Eul10d, the consideration of shear variation across longitudinal axis and the associated normal transverse stress components really provides the flexibility.

5.2 Free vibration analysis

In this subsection, the free vibration analysis results are validated against the results available in published literature. Consistent as well as Lumped mass models were considered in the free vibration analysis. The results obtained using consistent model are represented with Eul4d(C), Eul10d(C) and results through lumped mass model are represented with Eul4d(L), Eul10d(L).

5.2.1 Cantilever beam with metallic face sheets

For free vibration problem, a thin sandwich cantilever beam composed of two isotropic face sheets and a flexible core is investigated. Details of beam are given in Table 3.

The obtained results are compared with the results based on other theories, available in published literature and the results for first 5 modes are presented in Table 4. The number of elements used in the present work is 15 as used by other researchers such as Ahmed (1971) and Mead and Sivakumaran (1961) in their respective works. Ahmed (1971) had put forward three displacement models incorporating an element having 3, 4 and 5 degrees of freedom per node for modeling the curved sandwich beams with a general assumption that the material is elastic and homogeneous and the transverse displacement does not vary through thickness of the sandwich beam. Results by Mead and Sivakumaran (1961) are based on the Stodala method. Hwu *et al*. (2004), presented a close form solution for an identical free vibration problem and derived an orthogonal relation taking into account the effects of rotary inertia and shear deformation. Marur and Kant (1996) have reported results using Timoshenko theory and Higher Order Beam Theories (HOBT), namely HOBT4a, HOBT4b (both 4 degrees of freedom per node) and HOBT5 (5 degrees of freedom per node). But the results using HOBT5 element

Table 4 Comparison of frequencies-Cantilever beam, Frequencies in Hz

Mode	1	2	3	4	5
Timo (Marur 1996)	33.60	195.00	492.00	857.00	1260.00
HOBT5 (Marur 1996)	33.70	197.50	505.50	890.50	1231.00
Ahmed (Ahmed 1971)	32.80	193.50	499.00	886.00	1320.00
Mead (Mead 1961)	34.20	201.85	520.85	925.40	1381.30
C Hwu (Hwu 2004)	32.00	193.00	509.00	923.00	1402.00
Eul4d (C)	33.63	198.15	510.48	904.97	1346.80
Eul10d (C)	33.64	198.20	510.14	902.49	1338.80
Eul4d (L)	33.56	196.35	501.85	880.14	1291.60
Eul10d (L)	33.55	196.06	499.82	873.18	1274.80

Table 5 Comparison of frequencies-SS beam, Frequencies(Hz)

Mode	1	2	3	4	5
Timo (Marur 1996)	57.00	216.00	452.00	736.00	1054.00
HOBT5 (Marur 1996)	57.00	218.00	461.00	759.00	1097.00
Ahmed (Ahmed 1971)	55.50	-	451.00	-	1073.00
Exact (Chen 1961)	57.48	220.68	467.00	770.00	1108.50
C Hwu (Hwu 2004)	54.00	212.00	457.00	770.00	1130.0
Eul4d (C)	56.93	218.44	461.88	761.66	1096.70
Eul10d (C)	56.94	218.49	461.56	758.90	1086.80
Eul4d (L)	56.84	217.01	454.97	741.04	1049.50
Eul10d (L)	56.84	216.91	454.08	737.10	1038.10

only were considered for study.

The exact solution for fundamental frequency of a cantilever sandwich beam by Backstrom and Nilson (2007) is given as $\left(\frac{1.875}{l}\right)^2\sqrt{\frac{D}{\mu}}$, where D is the bending stiffness, (which is equal to $E_t\,I_t + E_b\,I_b$) and μ is mass per unit area of the homogenous beam(which is equal to $\frac{lb\,(\rho_t h_t + \rho_b h_b + \rho_c h_c)}{lb}$. As per this expression, the fundamental frequency of the present cantilever sandwich beam is 33.75 Hz and the results obtained using the formulated elements are matching closely. In the present work, the frequencies are computed using both consistent and lumped mass models and the results obtained are presented in Table 4.

5.2.2 Simply supported beam with metallic face sheet

Next, the beam considered here is same as what was studied in last section, the properties of which is given in Table 3 except that the length l is assumed as $0.9144m$. For this example, exact solution was referred by Chen et *al.* (2003), and the frequencies obtained are compared with the results that are obtained with other theories explained in the last example. Table 5 shows the comparison of results. We can clearly see that the results predicted by the present elements is very close to the exact results given by Chen *et al.* (2003), compared to other theories. Referring to Backstrom and Nilson (2007), the expression for exact solution for fundamental frequency of a simply supported sandwich beam is given as $\left(\frac{\pi}{l}\right)^2\sqrt{\frac{D}{\mu}}$,, where D is the bending stiffness,(which is equal to $E_t\,I_t + E_b\,I_b$) and μ is mass per unit area of the homogenous beam which is equal to $\frac{lb\,(\rho_t h_t + \rho_b h_b + \rho_c h_c)}{lb}$. As per this expression, the fundamental frequency of the present simply supported sandwich beam is 57.3778 Hz and the results obtained using the formulated elements are matching closely.

Table 6 SS Sandwich beam with composite face sheet

Material properties
Face sheets: Quasi-isotropic glass ceramic composite Young's modulus (E_f): 36000 N/ mm^2 Mass density (ρ_f): 4400 kg/m^3 Core: Isotropic Polymethacrylimide rigid foam Shear modulus (G_c) 20 N/mm^2 Mass density(ρ_c) 52.06 kg/m^3
Geometry Details
Length 'l', width 'b': 300 mm, 20 mm h_t, h_b, h_c: $0.5\ mm, 0.5\ mm\ , 20\ mm$

Table 7 Comparison of Frequency (Hz) Results for SS beam

Yang,Qiao model A*	Yang,Qiao model B*	Frostig,Baruch model B*	ABAQUS*
362.96	325.98	325.98	349.86

*[Yang *et al.* (2005)]

Eul10d model A	Eul4d model A	Eul10d model B	Eul4d model B
359.12	358.38	322.94	322.28

In both test cases above, it can be noticed that the frequencies obtained using both consistent and lumped mass models are predicting closer and accurate values in both Eul4d and Eul10d elements.

Following observations can be made based on the results.

• It can be observed from Tables 4 and 5, that the results predicted by Eul4d and Eul10d elements in both the models are matching well with other theories.

• It can be observed that the values predicted by consistent model are on higher side, as expected for both the elements. It is also can be noted down that the values predicted by Eul4d are higher than Eul10d element in both the models.

• The frequencies predicted using lumped mass are matching very closely with Timoshenko model and HOBT5 theories. The results indicate that the frequencies computed using lumped mass model are matching more closely with Timoshenko model (Ahmed 1971). The second and third modes predicted with the present theory are matching well, but are very close to HOBT5, Mead and Hwu results. Higher modes predicted using present theory are slightly higher than that of Timoshenko while they are very close to those predicted by Mead and Hwu.

It can be noted down that the formulated elements are not only able to predict the results close to many higher order theories, but also able to do so using smaller number of elements.

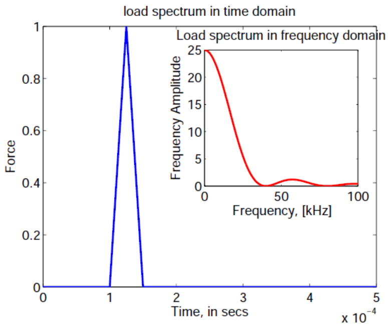

Fig. 8 Triangle pulse Load diagram

5.2.3 Simply supported beam with composite face sheet

To study the dynamic effects of core, a simply supported sandwich beam with composite face sheets, whose properties are given in Table 6 is considered. The focus of this example is to illustrate the ability to incorporate the dynamic effects of the core while carrying out the free vibration analysis. The natural frequencies are obtained for two cases namely

i) model A: the dynamic effects of core are neglected.

ii) model B: dynamic effects of core are included.

The results of fundamental frequencies predicted by the developed elements (with 20 elements)- Eul10d, Eul4d and are compared with the results obtained by Yang and Qiao (by using the series solution), FE solution using ABAQUS (face sheets are modelled using 2-D elements and core is modelled with 3-D elements) reported by Yang *et al.* (2005), and the results obtained by Frostig and Baruch, based on higher order theory

The constitutive models assumed for the present elements are close to the theories proposed by Yang *et al.* One can notice that the frequencies predicted by various theories in model A and model B differ significantly, which is due to the dynamic effects of core. In FE *ABAQUS* model, sandwich beams are modeled with 2D elements for face sheets and 3D elements for core. Generally, 2D elements as against beam elements for face sheets and 3D elements for core will make the sandwich beam stiffer and also introduce the incompatibility in slope/rotation between 2D bending and 3D elements, may contribute lesser energy transfer between the face sheets and core. Hence, the frequencies obtained using FE analysis in *ABAQUS* are on higher side when compared to the similar model B results.

Following observations can be made based on the results.

• Yang, Qiao results for model A are matching with FE results predicted by ABAQUS while Yang and Qiao results for model B are matching with Frostig, Baruch.

• Eul10d model A results are matching closely with the Yang, Qiao model A results and FE results predicted by *ABAQUS*.

• Results of Eul10d, Eul4d elements for model B are matching closely with the corresponding results by Yang, Qiao and Frostig, Baruch (model B)

In FE model, sandwich beams are modeled with 2D elements for face sheets and 3D elements for core. Generally, 2D elements against beam elements for face sheets and 3D elements for core will make the sandwich beam stiffer and also the incompatible slope/rotation between 2D bending and 3D elements may contribute to lesser energy transfer between the face sheets and core. Hence, the frequencies obtained using FE analysis in ABAQUS are on higher side when compared to the similar model B results.

It can be noticed that the frequencies predicted for present developed elements match closely with the results referred above for the cases with and without dynamic effects of core. Hence, it is evident that the elements developed can be used for predicting the fundamental frequencies of the sandwich beams accurately.

Table 8 Details of sandwich beam taken for Wave propagation studies

Material properties
Face sheets: *Aluminium* $E_t = E_b = 68E3\ Mpa, \quad \rho_t = \rho_b = 2683\ Kg/m^3$ *Core*: *Calcium Alginate* $G_c = 82.764\ Mpa\ , \rho_c = 32.8381\ Kg/m^3$
Geometry Details
Length ‘l’, width ‘b’: 1000 mm, 20 mm h_t, h_b, h_c: 2 mm, 2 mm , 20m m

6. Wave propagation analysis

In all wave propagation problems, a large number of modes contribute to the dynamic response and very high frequency content of the exciting force is needed to excite all the higher modes. From the view point of FE analysis, this requires the element size to match with the wavelength and hence very fine mesh discretization is generally adopted. In this context, the super convergence property of element gives an advantage to analyze the wave propagation problems with less number of elements. Element size in FE analysis can be decided based on the wavelength of the wave that can traverse the structure as well as the frequency content of the signal. Typically, it requires nearly 6 to 10 elements to model a wavelength. This section outlines the details of wave propagation studies carried out using super convergent finite elements developed in this paper and the validation of results obtained using *NASTRAN*.

A cantilever beam subjected to impact load, as shown in Fig. 8, applied in longitudinal and transverse directions at top face at free end, is chosen as a test case and the geometric, material properties are given in Table.8. In this case, the load duration is about 50 micro seconds and frequency of loading, ω is $\left(\frac{2\pi}{50}\right)10^6$ cycles per sec, longitudinal wave speed is given as $c=\sqrt{\frac{E_t}{\rho_t}}$ and wavelength is given by $\delta = \frac{2\pi c}{\omega}$, which is calculated as 8 mm approximately. In order to capture such wavelength, the number of elements required to model the length are in the range of 600 to 1000. While the number of super convergent FE required will be much lesser from 40 to 100

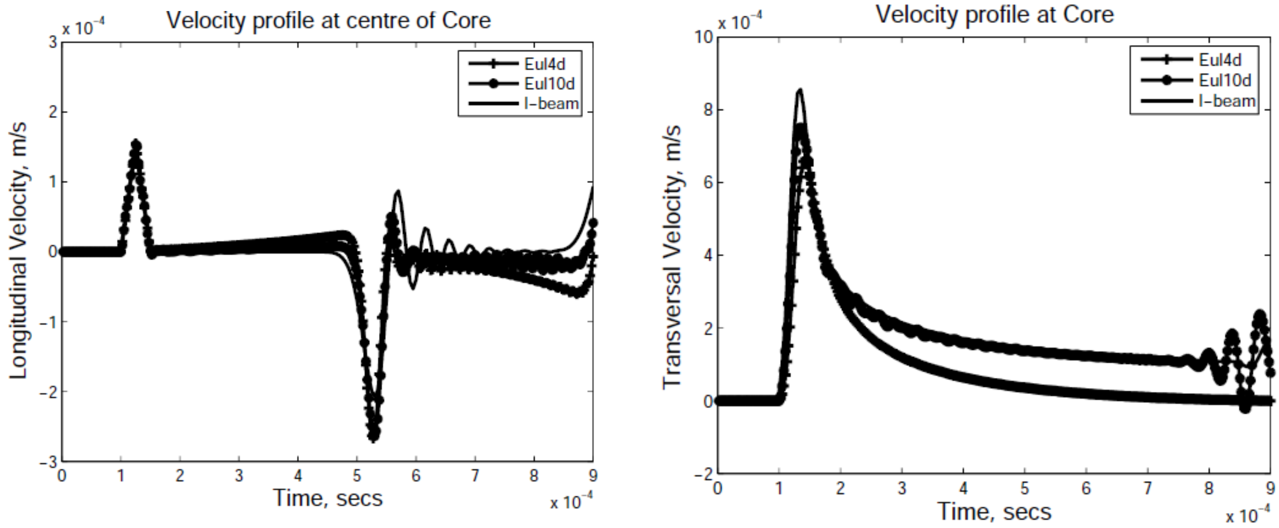

(a) Longitudinal velocity response (b) Transverse velocity response

Fig. 9 Transient responses for a typical I beam at mid core

as the displacement functions are higher order and the stiffness is accurate.

As the bending or transverse waves are highly dispersive, the wave speed changes with frequency. Lower frequency components travel slower. Hence, they appear late in the time window as opposed to higher frequency components, which travel fast and appear earlier in the chosen time window. Using the broad band signal, as chosen in this example, excites many higher order bending modes and hence 100 formulated elements are used to model this problem. Analysis has been carried out using Newmark time marching scheme and for this case a time step,($\Delta\, t$) of 1 μ sec is used. The responses are measured at the free end tip of the top and the bottom face sheets. For comparison, the same configuration is analysed using *NASTRAN*, a general-purpose Finite element software, for undamped condition in the dynamic analysis. Direct Integration Method is used for the analysis in *NASTRAN*.

6.1 Validation using homogenous I beam

In this study, all the super convergent FE sandwich beam elements developed (Eul10d and Eul4d) are considered. First, validation of the results under transient load as shown in Fig. 8 is carried out, where the load is acting in longitudinal and transverse directions separately. For this validation, the same beam is assumed with I cross section by considering the equivalent material properties. This means that the beam is homogenous with geometrical properties of $h_t = 2\,mm, h_b = 2\,mm,\ h_c = 20\,mm.$ In *NASTRAN*, *I* beam cross section is defined while the discretization of the beam was carried out using 1000 beam elements. The loads and boundary conditions are applied at the element node line which is the center line of core, while they are actually applied at the top and the bottom face sheets, in case of Eul10d. In case of Eul4d, they will act at center line of the core.

The velocity responses obtained with the elements developed in the present work and *NASTRAN I* beam are compared. In order to simulate the loads application closely with actual case, the loads in case of Eul10d are applied at the top and the bottom face sheets, distributed equally. As the loads and boundary conditions are symmetric, the velocity responses at top and bottom face sheets are expected to be same. Hence, only the results obtained at the top face sheet are compared with NASTRAN results as the part of validation.

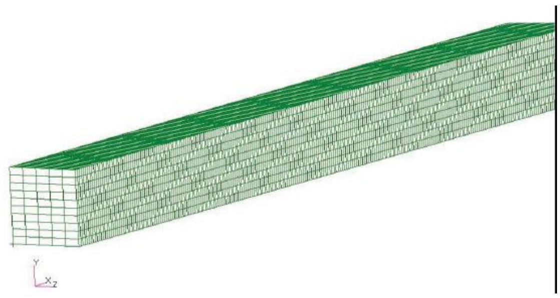

Fig. 10 Discretization of the sandwich beam

The longitudinal velocity responses, when the beam is subjected to the transient load applied in the longitudinal direction and the transverse velocity response under the loads in the transverse direction are presented in Fig. 9. From Fig. 9, it can be observed that the longitudinal and transverse velocity responses obtained using Eul4d and Eul10d matches closely with the *NASTRAN I* beam results. The results show that the formulated elements are able to predict the reflection away due to fixed boundary, accurately for the both cases. That is, this example shows that, one can use homogenous beam assumption to obtain responses of the hybrid sandwich structure.

The wave is expected to travel a distance of 1 m forward, 1m backward with a speed of 5000 m/s and hence, the first reflection is expected after 0.0004 seconds since the application of loading. The first longitudinal reflection is predicted around 525 μ seconds and second reflection around 925 μ seconds. The longitudinal response predicted by *NASTRAN* '*I*' beam represents a wavy nature which is

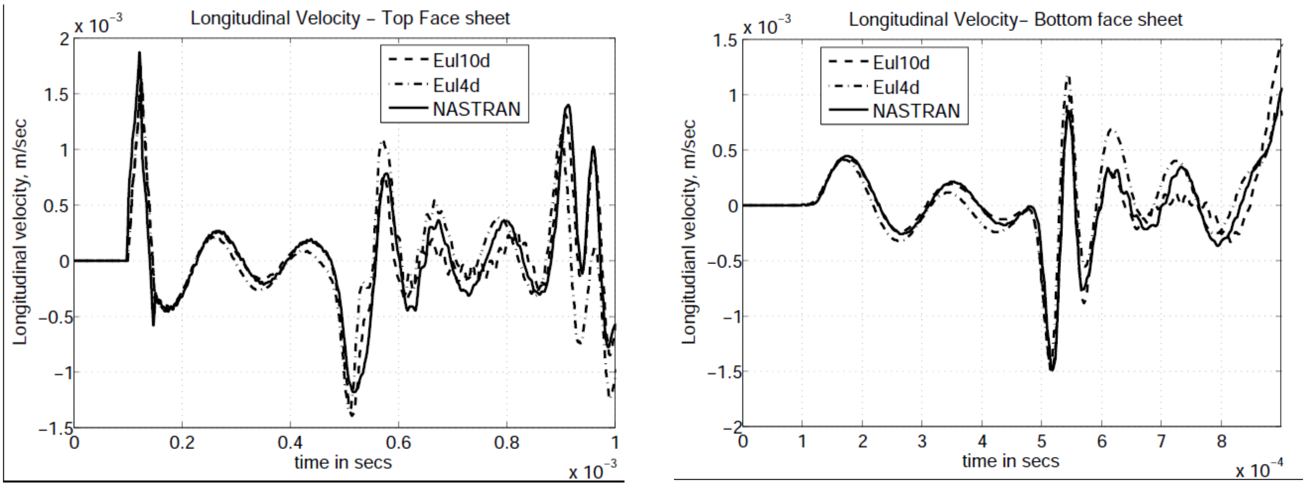

(a) At top face sheet, V_l^t

(b) At bottom face sheet, V_l^b

Fig. 11 Transient response-Longitudinal velocities

due to approximation mode in the analysis. One can perform similar analysis to predict results from the formulated element for transverse loading to show that the predictions of formulated element as opposed to *NASTRAN I* beam results are very accurate. Next, we use the formulated elements for the case of sandwich beam with soft core and asses their performance.

6.2 Sandwich beam with soft core

Modeling of sandwich beams is possible in *NASTRAN*, in multiple ways, by using different elements for the face sheets and core. Combination of different set of elements for face sheets and core will simulate the corresponding kinematics for sandwich beams, some will result in rigid core, some will represent the flexible core with high or moderate stiff face sheets. This kinematics will hold the key in obtaining the transient responses according to the modes that it can simulate. Face sheets can be modeled with bending elements, CBEAM in 1D, CQUAD4 in 2D and CHEXA in 3D while the core with shear elements, namely CSHEAR, CQUAD Shear in 2D and CHEXA in 3D. CSHEAR and CQUAD4 shear elements generally represents pure shear elements and it will not consider any bending in the core. In case of the use of different elements for face sheets and core, the kinematics compatibility at the interface simulated will cause the responses accordingly. In the present study, the model with CHEXA for face sheets as well as the core is used to avoid all compatible expected with combination of elements, although it requires more elements and consumes more computer time. As 3d CHEXA elements are used to model, the responses are preliminary controlled by the in-plane stiffness and are represented through the deformations.

In order to ensure proper core action, about ten layers of CHEXA elements are used for modeling of core across its depth. FE mesh comprises total number of CHEXA elements about 140000 with total number of nodes about 168614 and total degrees of freedom about 448380. The mesh is as shown in Fig. 10.

The longitudinal velocity response at top and bottom face sheets obtained under the unit load applied in longitudinal direction on top face sheet are presented in Fig. 11. Transverse velocity profile, when a unit load is applied in the transverse direction, at top and bottom face sheets are plotted in Fig. 12. Figs. 11(a), (b) shows the comparison of longitudinal velocity responses. and Figs. 12(a), (b) shows the comparison of transverse velocity responses. Among all models, the response predicted by Eul4d is on higher side as it is lower order element with incompressible effects of core and hence the energy capture between the face sheets and core will not be full.

Following are the observations that can be made based on the results.

• The longitudinal velocity response at top and bottom face sheets, V_l^t and V_l^b shows close match between the predictions made by Eul4d, Eul10d and NASTRAN. The velocity profiles predicted by all are similar and different from a simple beam. Wavy nature seen in the response curves due to the interactions through σ_{zz}^c and τ_{xz}^c due to their approximations in the model. All models have predicted the reflections accurately.

• The velocity response predicted at top face sheet, V_l^t, at 125 μ seconds during transient state, by Eul4d, Eul10d and *NASTRAN* at top face sheet are about $1.65, 1.650$ and 1.85 mm/s. While at bottom face sheet, the responses V_l^b are about $0.40, 0{,}40$ and 0.45 mm/s.

• As expected, CHEXA predicts are on higher side while compared to Euler elements due to the lesser stiffness considerations.

• The transverse velocity response, V_t^t, predicted during the transient phase at 125 μ seconds by Eul4d, Eul10d and *NASTRAN* are about $4.2, 5.25, 8.5$mm/s. Response predicted by Eul4d and Eul10d are matching closely although the response by Eul10d is wavy. It is due to the presence of σ_{zz}^c. The response predicted by Eul4d are the same throughout depth of core, which can be considered at mid core.

• The response predicted at bottom face sheet, V_t^b, by Eul10d and *NASTRAN* are about $3.0, 1.3$ mm/s respectively. As Eul4d has transverse displacement same

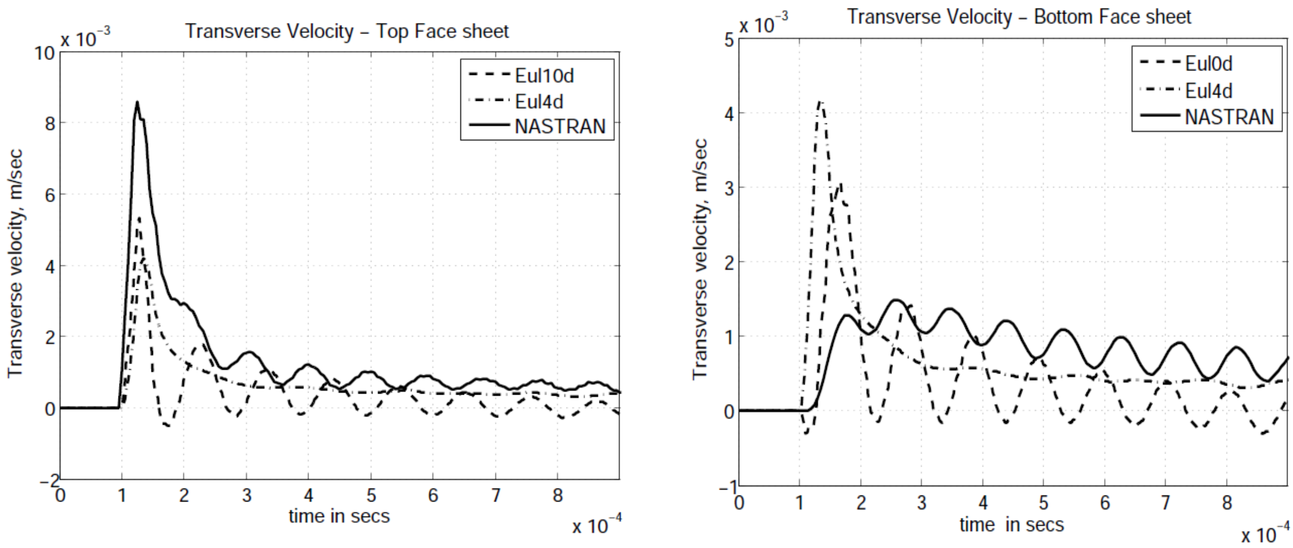

(a) At top face sheet, V^t_{t} (b) At bottom face sheet V^b_{t}

Fig. 12 Transient response-Transverse velocities

throughout the core, both V_t^t, V_t^b are same.

• If the average of these responses at top and bottom face sheets for Eul10d and *NASTRAN* are computed, they can be approximately 4.10, 4.9 mm/s while response predictions by Eul4d are 4.2 mm/s. This which clearly brings out that the response predictions on overall beam as a whole are matching well and the distribution internally is different in models.

It is necessary to bring out an important aspect of the use of time and computer resources for analysis. As *NASTRAN* model has considerable degrees of freedom, it has taken considerable time, in hours while the developed elements require fraction of seconds for analysis on same computer. It is proved with the current study that the elements developed are accurate for wave propagation studies, which are key in health monitoring studies and also computationally efficient, takes less time to solve with lesser resources.

7. Conclusions

This paper presented the necessity of having accurate, powerful finite elements for modeling sandwich beams with metallic or composite face sheets and soft material cores. The following conclusions can be made from this paper.

• Super convergent sandwich finite beam elements Eul10d and Eul4d based on the Euler Bernoulli Beam theory, compressible and incompressible rigid core were developed.

• Formulation of super convergent sandwich beam elements were presented along with their development of stiffness and mass matrices.

• The performance of the developed elements is thoroughly validated under static loads and free vibration for the sandwich beams with metallic as well as composite face sheets.

• The extensive detailed studies carried out show that the results predicted by these elements are closer to the results predicted by higher order theories using only a smaller set of unknowns. Therefore, these elements developed demonstrated their super convergence property. This is due to exact representation of beam stiffness in the formulation.

• Later, the wave propagation analysis under impact load is dealt with and the advantages of this element for its computational efficiency is demonstrated by its ability to capture wave responses at a fraction of computational cost, which can be clearly seen from the wave propagation studies.

• Super convergent sandwich beam finite elements are proved for their accuracy and performance which is presented in the paper. They are recommended for their use in the industry for the analysis while designing them.

• Super Convergent elements Eul4d and Eul10d can be used to carry out the analysis of sandwich beams for the design of sandwich beams.

Acknowledgments

The authors are grateful to Aeronautical Development Agency, Ministry of Defence, Bangalore for carrying out the work and permission to publish in this journal.

References

Frostig, Y. (2003), "Classical and higher order computational models in the analysis of modern sandwich panels", *Compos. Part B*: *Eng*., **34**, 83-100.

Frostig, Y. (1992), "Behavior of delaminated sandwich beam with transversely flexible core-high order theory", *Compos. Struct*., **20**, 1-16.

Frostig, Y. and Baruch, M. (1994), "Free vibrations of sandwich beams with a transversely flexible core: A higher order approach", *J. Sound Vibr*., **176**(2), 195-208.

Marur, S.R. and Kant, T. (1996), "Free vibration analysis of fiber reinforced composite beams using higher order theories and

finite element modeling", *J. Sound Vibr*., **194**(3), 337-351.
Zhen, W. and Wanji, C. (2008), "An assessment of several displacement-based theories for the vibration and stability analysis of laminated composites and sandwich beams", *Compos. Struct*., **84**(4), 337-349.
Yang, M. and Qiao, P. (2005), "Higher order impact modelling of sandwich structures with flexible core", *J. Sol. Struct*., **42**, 5460-5490.
Yang, M. and Qiao, P. (2007), "Impact and damage prediction of sandwich beams with flexible core considering arbitrary boundary effects", *J. Sandw. Struct. Mater*., **9**(5), 411-444.
Catherine, N.P., Yeoshua, F. and George, A.K. (2012), "Analysis of sandwich beams with a compliant core and with in-plane rigidity-extended high-order sandwich panel theory versus elasticity", *J. Appl. Mech*., **79**(4).
Li, X.Y. and Liu, D. (1997), "Generalised laminate theories based on double superposition hypothesis", *J. Numer. Meth. Eng*., **40**, 1197-212.
Cho, M. and Parmerter, R. (1993), "Efficient higher order composite plate theory for general lamination configurations", *AIAA J*., **31**, 1299-1306.
Marco, G. (2013), "On the use of zigzag functions in equivalent single layer theories for laminated composite and sandwich beams: A comparative study and some observations on external weak layers", *J. Appl. Mech*., **80**(6).
Matsunaga, H. (2001), "Vibration and buckling of multi layered composite beams according to higher order deformation theories", *J. Sound Vibr*., **246**, 47-62.
Kant, T. and Swaminathan, K. (2001), "Analytical solutions for free vibrations of laminated composite and sandwich plates based on a higer order refined theory", *Compos. Struct*., **53**, 73-85.
Reddy, J.N. (1984), "A Simple higher order theory for laminated composite plates", *J. Appl. Mech*., **51**, 745-752.
Damanpacka, A.R. and Khalilia, S.M.R. (2012), "High-order free vibration analysis of sandwich beams with a flexible core using dynamic stiffness method", *Compos. Struct*., **94**(5), 1503-1514.
Inés, I., Carlos, S. and Sonia, S.S. (2010), "FEM analysis of dynamic flexural behaviour of composite sandwich beams with foam core", *Compos. Struct*., **92**(9), 2285-2291.
Gillich, G.R., Praisach, Z.I., Abdel Wahab, M. and Vasile, O. (2014), "Localization of transversal cracks in sandwich beams and evaluation of their severity", *Shock Vibr*., **607125**, 10.
Wang, Z., Jing, L., Ning, J. and Zhao, L. (2011), "The structural response of clamped sandwich beams subjected to impact loading", *Compos. Struct*., **93**(4), 1300-1308.
Banerjee, J.R., Cheung, C.W., Morishima, R., Perera, M. and Njuguna, J. (2007), "Free vibration of a three-layered sandwich beam using the dynamic stiffness method and experiment", *J. Sol. Struct*., **44**, 7543-7563.
Tagarielli, V.L., Deshpande, V.S. and Fleck, N.A. (2010), "Prediction of the dynamic response of composite sandwich beams under shock loading", *J. Imp. Eng*., **37**(7), 854-864.
Poortabib, A. and Maghsoudi, M. (2014), "The analytical solution for buckling of curved sandwich beams with a transversely flexible core subjected to uniform load", *Struct. Eng. Mech*., **52**(2).
Mohammadimehr, M. and Shahedi, S. (2016), "Nonlinear magneto-electro-mechanical vibration analysis of double-bonded sandwich Timoshenko microbeams based on MSGT using GDQM", *Steel Compos. Struct*., **21**(1).
Yan, J.B., Liew, J.Y.R. and Zhang, M.H. (2015), "Ultimate strength behavior of steel-concrete-steel sandwich beams with ultra-lightweight cement composite, part 2: Finite element analysis", *Steel Compos. Struct*., **18**(4).
Yusuf, C. (2015), "Free vibration analysis of edge cracked symmetric functionally graded sandwich beams", *Struct. Eng. Mech*., **56**(6).
Noureddine, E.M., Tounsi, A., Ziane, N., Mechab, I. and Adda Bedia, E.A. (2011), "A new hyperbolic shear deformation theory for buckling and vibration of functionally graded sandwich plate", *J. Mech. Sci*.
Mohamed Ait Amar, M., Hadj, H.A. and Abdelouahed, T. (2014), "An efficient and simple refined theory for buckling and free vibration of exponentially graded sandwich plates under various boundary conditions", *J. Sandw. Struct. Mater*., **16**(3), 293-318.
Houari, M.S.A., Tounsi, A., Bessaim, A. and Mahmoud, S.R. (2016), "A new simple three-unknown sinusoidal shear deformation theory for functionally graded plates", *Steel Compos. Struct*., **22**(2), 257-276.
Boukhari, A., Atmane, H.A., Tounsi, A., Adda Bedia, E.A. and Mahmoud, S.R. (2016), "An efficient shear deformation theory for wave propagation of functionally graded material plates", *Struct. Eng. Mech*., **57**(5), 837-859.
Hichem, B., Kouider, H.B., Hadji, L., Mohammed, S.A.H. and Abdelouahed, T. (2016), "Bending and free vibration analysis of functionally graded plates using a simple shear deformation theory and the concept the neutral surface position", *J. Braz. Soc. Mech. Sci. Eng*., **38**(1), 265-275.
Hadj, H.A., Hassen, A.A., Ismail, M., Lakhdar, B., Abelouahed, T., Adda Bedia, E.A. (2011), "Static analysis of functionally graded sandwich plates using an efficient and simple refined theory", *Chin. J. Aeronaut*., **24**(4), 434-448.
Hadj, H.A., Mohamed, A.A.M., Abdelmoumen, A.B., Abdelouahed, T., Mahmoud, S.R. and Afaf, S.A. (2017), "An efficient hyperbolic shear deformation theory for bending, buckling and free vibration of FGM sandwich plates with various boundary conditions", *Steel Compos. Struct*., **25**(6), 693-704.
Malekzadeh Fard, K. (2014), "Higher order free vibration of sandwich curved beams with a functionally graded core", *Struct. Eng. Mech*., **49**(5).
Atmane, H.A., Tounsi, A., Bernard, F. and Mahmoud, S.R. (2015), "A computational shear displacement model for vibrational analysis of functionally graded beams with porosities", *Steel Compos. Struct*., **19**(2), 369-384.
Yahia, S.A., Atmane, H.A., Houari, M.S.A. and Tounsi, A. (2015), "Wave propagation in functionally graded plates with porosities using various higher-order shear deformation plate theories", *Struct. Eng. Mech*., **53**(6), 1143-1165.
Lazreg, H., Zoubida, K. and Adda Bedia, E.A. (2016), "A new higher order shear deformation model for functionally graded beams", *KSCE J. Civil Eng*., **20**(5), 1835-1841.
Habib, H., Abdelouahed, T., Mohammed, S.A.H. and Aicha, B. (2014), "A new quasi-3D hyperbolic shear deformation theory for the static and free vibration analysis of functionally graded plates", *ASCE J. Eng. Mech*., **140**, 374-383.
Zakaria, B., Mohammed, S.A.H., Abdelouahed, T., Mahmoud, S.R. and Anwar Bég, O. (2014), "An efficient and simple higher order shear and normal deformation theory for functionally graded material (FGM) plates", *Compos.: Part B*, **60**, 274-283.
Amale, M.E., Abbas Adda, B. and Abdelouahed, T. (2015), "A new hyperbolic shear deformation theory for bending and free vibration analysis of isotropic, functionally graded, sandwich and laminated composite plates", *Appl. Math. Model*., **39**, 2489-2508.
Bourada, M., Kaci, A., Houari, M.S.A. and Tounsi, A. (2015), "A new simple shear and normal deformations theory for functionally graded beams", *Steel Compos. Struct*., **18**(2), 409-423.
Bennai, R., Atmane, H.A. and Tounsi, A. (2015), "A new higher-order shear and normal deformation theory for functionally graded sandwich beams", *Steel Compos. Struct*., **19**(3).
Mohamm, M.B., Houari, M.S.A. and Tounsi, A. (2016), "A novel

five variable refined plate theory for vibration analysis of functionally graded sandwich plates", *Mech. Adv. Mater. Struct.*, **23**(4), 423-431.

Bounouara, F., Benrahou, K.H., Belkorissat, I. and Tounsi, A. (2016), "A nonlocal zeroth-order shear deformation theory for free vibration of functionally graded nanoscale plates resting on elastic foundation", *Steel Compos. Struct.*, **20**(2), 227-249.

Abdelouahed, T., Mohammed, S.A.H., Samir, B. and El Abbas, A.B. (2013), "A refined trigonometric shear deformation theory for thermoelastic bending of functionally graded sandwich plates", *Aerosp. Sci. Technol.*, **24**(1), 209-220.

Bouderba, B., Houari, M.S.A. and Tounsi, A. (2013), "Thermomechanical bending response of FGM thick plates resting on Winkler-Pasternak elastic foundations", *Steel Compos. Struct.*, **14**(1), 85-104.

Ahmed, H., Mohammed, S.A., Houari, S.R.M. and Abdelouahed, T. (2015), "A sinusoidal plate theory with 5-unknowns and stretching effect for thermomechanical bending of functionally graded sandwich plates", *Steel Compos. Struct.*, **18**(1), 235-253.

Bouderba, B., Houari, M.S.A., Tounsi, A. and Mahmoud, S.R. (2016), "Thermal stability of functionally graded sandwich plates using a simple shear deformation theory", *Struct. Eng. Mech.*, **58**(3), 397-422.

Abdelmoumen, A.B., Samir, B., Abdelouahed, T. and Mahmoud, S.R. (2016), "On thermal stability of plates with functionally graded coefficient of thermal expansion", *Struct. Eng. Mech.*, **60**(2), 313-335.

Chikh, A., Tounsi, A., Hebali, H. and Mahmoud, S.R. (2017), "Thermal buckling analysis of cross-ply laminated plates using a simplified HSDT", *Smart Struct. Syst.*, **19**(3), 289-297.

Fouzia, E.H., Bakora, A., Bousahla, A.A., Tounsi, A. and Mahmoud, S.R. (2017), "A simple analytical approach for thermal buckling of thick functionally graded sandwich plates", *Struct. Eng. Mech.*, **63**(5), 585-595.

Menasria, A., Bouhadra, A., Tounsi, A., Bousahla, A.A. and Mahmoud, S.R. (2017), "A new and simple HSDT for thermal stability analysis of FG sandwich plates", *Steel Compos. Struct.*, **25**(2), 157-175.

Hichem, B., Ahmed, B., Abdelouahed, T., Abdelmoumen, A.B. and Mahmoud, S.R. (2017), "An efficient and simple four variable refined plate theory for buckling analysis of functionally graded plates", *Steel Compos. Struct.*, **25**(3), 257-270.

Gopalakrishnan, S. (2000), "A deep rod finite element for structural dynamics and wave propagation problems", *J. Numer. Meth. Eng.*, **48**, 731-744.

Chakraborty, A., Mahapatra, D.R. and Gopalakrishnan, S. (2002), "Finite element analysis of free vibration and wave propagation in asymmetric composite beams with structural discontinuities", *J. Compos. Struct.*, **55**, 23-36.

Mitra, M., Gopalakrishnan, S. and Seetharam Bhat, M. (2004), "A new super convergent thin walled composite beam for analysis of box beam structures", *J. Sol. Struct.*, **41**, 1491-1518

Murthy, M.V.V.S., Mahapatra, D.R., Badarinarayana, K. and Gopalakrsihnan, S. (2005), "A refined higher order finite element for asymmetric composite beams", *Compos. Struct.*, **67**, 27-35.

Murthy, M.V.V.S., Gopalakrsihnan, S. and Nair, P.S. (2007), "New locking free higher order finite element formulation for composite beams", *J. Comput. Mater. Contin.*, **5**(1), 43-62.

Ghosh, D.P. and Goplakrishnan, S. (2007), "A super convergent finite element for composite beams with embedded magnetostrictive patches", *Compos. Struct.*, **79**, 315-330.

Sudhakar, G. and Vijayaraju. (2010), "Development of a new finite element for the analysis of sandwich beams with soft core", *J. Sandw. Struct. Mater.*, **12**, 649-683.

Backstrom, D. and Nilson, A.C. (2007), "Modelling the vibration of sandwich beams using frequency-dependent parameters", *J. Sound Vibr.*, **300**, 589-611.

Ahmed, K.M. (1971), "Free vibrations of curved sandwich beams by the method of finite elements", *J. Sound Vibr.*, **18**(1), 61-74.

Hwu, C. and Chang, W.C. and Gai, H.S. (2004), "Vibration suppression of composite sandwich beams", *J. Sound Vibr.*, **272**, 1-20.

Chen, W.Q., Lv, C.F. and Bian, Z.G. (2003), "Elasticity solution for free vibration of laminated beams", *Compos. Struct.*, **62**, 75-82.

Allen, H.G. (1969), *Sandwich Beams, Analysis and Design of Structural Sandwich Panels*, 1st Edition, Pergamon Press Ltd, London, U.K.

Gopalakrishnan, S., Chakraborty, A. and Mahapatra, D.R. (2008), *Spectral Finite Element Method*, Springer-Verlag, New York, U.S.A.

Cook, R.D. and Malkus, D.S. and Plesha, M.E. and Whitt, R.J. (2002), *Finite Elements in Structural Dynamics and Vibrations and Plate bending, Concepts and Applications of Finite Element Analysis*, 4th Edition, John Wiley and Sons (ASIA) Pte Ltd, Singapore.

Irving, H.S. and Clive, L.D. (2003), *Energy an Finite Element Methods in Structural Mechanics*, New Age International(P) Limited, Publishers.

Mario, P. (2001), *Structural Dynamics Theory and Computation*, CBS Publishers and Distributors, New Delhi, India.

Vinson, J.R. (1999), *The Behaviour of Sandwich Structures of isotropic and Composite Materials*, 1st Edition, Technomic Publishing Company, U.S.A.

Mead, D.J. and Sivakumaran, S. (1961), "The Stodala method applied to sandwich beam vibration", *Proceedings of the Symposium on Numerical Methods for Vibration Problems*, University of Southampton.

CC